

ASYMPTOTIC EXACTNESS OF THE LEAST-SQUARES FINITE ELEMENT RESIDUAL*

CARSTEN CARSTENSEN[†] AND JOHANNES STORN[‡]

Abstract. The discrete minimal least-squares functional $LS(f; U)$ is equivalent to the squared error $\|u - U\|^2$ in least-squares finite element methods and so leads to an embedded reliable and efficient a posteriori error control. This paper unfolds a spectral analysis to prove that this natural error estimator is asymptotically exact in the sense that the ratio $LS(f; U)/\|u - U\|^2$ tends to one as the underlying mesh-size tends to zero for the Poisson model problem, the Helmholtz equation, the linear elasticity, and the time-harmonic Maxwell equations with all kinds of conforming discretizations. Some knowledge about the continuous and the discrete eigenspectrum allows for the computation of a guaranteed error bound $C(\mathcal{T})LS(f; U)$ with a reliability constant $C(\mathcal{T}) \leq 1/\alpha$ smaller than that from the coercivity constant α . Numerical examples confirm the estimates and illustrate the performance of the novel guaranteed error bounds with improved efficiency.

Key words. least-squares finite element method, global upper bound, asymptotically exact error estimation, sharpened reliability constants, spectral analysis, Poisson model problem, Helmholtz equation, linear elasticity, Maxwell equations

AMS subject classifications. 65N12, 65N15, 65N30

DOI. 10.1137/17M1125972

1. Introduction. The least-squares finite element method (LSFEM) approximates the exact solution $u \in X$ to a partial differential equation by the discrete minimizer $U \in X(\mathcal{T})$ of a least-squares functional $LS(f; \bullet)$ over a discrete subspace $X(\mathcal{T}) \subset X$. For the problems in this paper, namely the Poisson model problem, the Helmholtz equation, the linear elasticity, and the Maxwell equations, the functional $LS(f; \bullet)$ is equivalent to the norm $\|\bullet\|_X^2$ in X with equivalence constants α and β . In particular, the discrete minimizer $U \in X(\mathcal{T})$ satisfies $\alpha \leq LS(f; U)/\|u - U\|_X^2 \leq \beta$ and the computable residual $LS(f; U)$ leads to a guaranteed upper bound (GUB) $\|u - U\|_X^2 \leq \alpha^{-1}LS(f; U)$ [3]. Table 1 displays computed upper and lower bounds of the quotient $LS(f; U)/\|u - U\|_X^2$ for a Poisson model problem and provides numerical evidence of asymptotic exactness of the least-squares residual $LS(f; U)$. This experiment suggests that the GUB $\alpha^{-1}LS(f; U)$ is too pessimistic for $\alpha^{-1} = 1.442114$.

The first main result of this paper verifies that the ratio $LS(f; U)/\|u - U\|_X^2$ with the unique exact (resp., discrete) minimizer u (resp., U) tends to one in the model problems from section 2 as the maximal mesh size δ of the underlying regular

*Received by the editors April 17, 2017; accepted for publication (in revised form) April 30, 2018; published electronically July 3, 2018.

<http://www.siam.org/journals/sinum/56-4/M112597.html>

Funding: The research of the first author was supported by the Deutsche Forschungsgemeinschaft in the Priority Program 1748 “Reliable simulation techniques in solid mechanics. Development of non-standard discretization methods, mechanical and mathematical analysis” under the project “Foundation and application of generalized mixed FEM towards nonlinear problems in solid mechanics” (CA 151/22-1). The research of the second author was supported by the Studienstiftung des deutschen Volkes.

[†]Corresponding author. Institut für Mathematik, Humboldt-Universität zu Berlin, D-10099 Berlin, Germany (cc@math.hu-berlin.de).

[‡]Institut für Mathematik, Humboldt-Universität zu Berlin, D-10099 Berlin, Germany (storn@math.hu-berlin.de).

TABLE 1

Guaranteed lower bounds (LB) and upper bounds (UB) for the quotient $LS(f; U) / \|u - U\|_X^2$ in the Poisson model problem with right-hand side $f \equiv 1$ on the L-shaped domain $\Omega = (-1, 1)^2 \setminus [0, 1)^2$ from subsection 5.1.

ndof	LB	UB	ndof	LB	UB
13	0.85367257	0.85996324	49153	0.99217867	1.00640795
49	0.93237486	0.94497564	196609	0.99522104	1.00419431
193	0.96674683	0.99157065	786433	0.99704395	1.00271554
769	0.98486169	1.01697465	3145729	0.99815838	1.00174352
3073	0.96995255	1.01406884	12582913	0.99884783	1.00111247
12289	0.98692470	1.00963924	50331649	0.99927741	1.00070662

triangulation \mathcal{T} , written $\mathcal{T} \in \mathbb{T}(\delta)$, tends to zero:

$$(1) \quad \forall \varepsilon > 0 \exists \delta > 0 \forall \mathcal{T} \in \mathbb{T}(\delta) \quad (1 - \varepsilon) \|u - U\|_X^2 \leq LS(f; U) \leq (1 + \varepsilon) \|u - U\|_X^2.$$

One key observation is that ε and δ are independent of the right-hand side f in $L^2(\Omega)$ and do *not* depend on the polynomial degrees of a balanced or unbalanced conforming discretization (but certainly depend on the domain and the parameters in the differential operators). To the best of the authors' knowledge, this is the first result of the asymptotically exact error estimation for those problems with standard discretizations; the results in [8] are caused by an unbalanced discretization. The proof of (1) in section 3 utilizes a spectral decomposition of the ansatz space X and the Galerkin orthogonality of the error $u - U$. The asymptotic exactness result implies the overestimation of $\|u - U\|_X^2$ by the natural GUB $\alpha^{-1}LS(f; U)$ with the factor $\alpha^{-1} > 1$ as the maximal mesh-size tends to zero. The second aim of this paper is to overcome this inefficiency by an (offline) improvement of the reliability constant $C(\mathcal{T})$ with $\|u - U\|_X^2 \leq C(\mathcal{T})LS(f; U)$ in a GUB (displayed in Figure 1), which captures the convergence of the least-squares residual to the exact error. Section 4 combines a priori knowledge of the continuous eigenspectrum with additional information on the discrete eigenspectrum and achieves a computable constant $C(\mathcal{T})$. The proof utilizes the Galerkin orthogonality of the discrete solution U and so the GUB requires an exact solve but is independent of the data f ; i.e., the constant $C(\mathcal{T})$ depends only on \mathcal{T} and $C(\hat{\mathcal{T}}) \leq C(\mathcal{T})$ for any refinement $\hat{\mathcal{T}}$ of \mathcal{T} even with polynomial enrichment of the discrete ansatz space $X(\hat{\mathcal{T}})$. A three-stage algorithm leads in subsection 4.2 to $C(\mathcal{T})$ and a significant improvement of the GUB $\alpha^{-1}LS(f; U)$, which is up to 132 times larger than $C(\mathcal{T})LS(f; U)$ in Figure 1. Further numerical experiments in section 5 on the Laplace, Helmholtz, and Maxwell equations investigate the improvement in computational benchmarks: Once the relevant eigenfunctions of the least-squares system are resolved with sufficient accuracy, the novel reliability constant $C(\mathcal{T})$ leads to a significant improvement of the GUB. The relevant eigenmodes are of low frequency in the Poisson and elasticity problems, while certain parameters of ω in the Helmholtz and Maxwell equations might lead to relevant high-frequency eigenmodes solely resolved for very fine meshes.

Standard notation on Lebesgue and Sobolev spaces applies throughout this paper, $H^1(\Omega) := \{v \in L^2(\Omega; \mathbb{R}) : \nabla v \in L^2(\Omega; \mathbb{R}^d)\}$, $H_0^1(\Omega) := \{v \in H^1(\Omega) : v|_{\partial\Omega} = 0\}$, $H(\operatorname{div}, \Omega) := \{q \in L^2(\Omega; \mathbb{R}^d) : \operatorname{div} q \in L^2(\Omega; \mathbb{R})\}$, and, for $d = 3$ only, $H(\operatorname{curl}, \Omega) := \{F \in L^2(\Omega; \mathbb{R}^3) : \operatorname{curl} F \in L^2(\Omega; \mathbb{R}^3)\}$, $H_0(\operatorname{curl}, \Omega) := \{F \in H(\operatorname{curl}, \Omega) : \nu \times F = 0 \text{ on } \partial\Omega\}$ with outer unit normal vector $\nu \in \mathbb{R}^3$.

2. Four applications of the LSFEM. This section introduces the model problems and their finite element discretizations for a bounded polyhedral Lipschitz do-

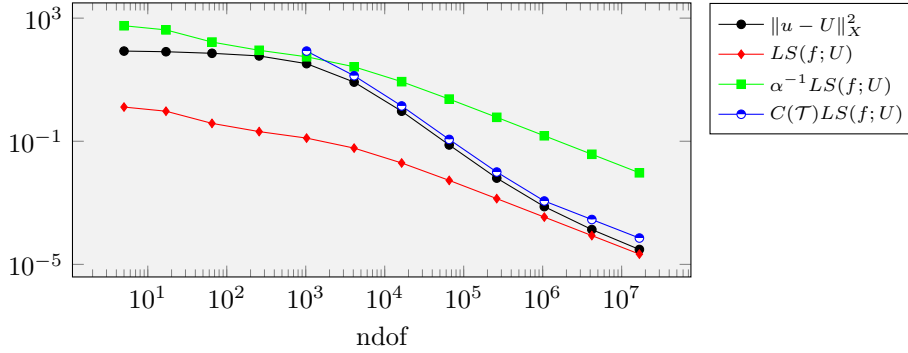


FIG. 1. Convergence history plot from subsection 5.4 of the squared error, residual, and GUB for the Helmholtz equation with $\omega = 4$.

main $\Omega \subset \mathbb{R}^d$.

2.1. Poisson model problem. Given $f \in L^2(\Omega; \mathbb{R})$, the Poisson model problem seeks $(u, p) \in X := H_0^1(\Omega) \times H(\operatorname{div}, \Omega)$ with

$$-\operatorname{div} p = f \text{ in } \Omega \quad \text{and} \quad \nabla u = p \text{ in } \Omega.$$

First-order systems least-squares (FOSLS) methods such as, e.g., those in [2, 10, 18, 20] utilize the equivalence of the Poisson model problem to the minimization of the least-squares functional

$$LS(f; v, q) := \|q - \nabla v\|_{L^2(\Omega)}^2 + \|f + \operatorname{div} q\|_{L^2(\Omega)}^2$$

over all $(v, q) \in X$ with norm $\|(v, q)\|_X^2 := \|\nabla v\|_{L^2(\Omega)}^2 + \|q\|_{L^2(\Omega)}^2 + \|\operatorname{div} q\|_{L^2(\Omega)}^2$.

2.2. Helmholtz equation. Given some $f \in L^2(\Omega; \mathbb{R})$ and a frequency $\omega^2 > 0$ different from a Dirichlet eigenvalue of the Laplace operator, the Helmholtz equation seeks $(u, p) \in X := H_0^1(\Omega) \times H(\operatorname{div}, \Omega)$ with

$$-\operatorname{div} p - \omega^2 u = f \text{ in } \Omega \quad \text{and} \quad \nabla u = p \text{ in } \Omega.$$

This problem is well posed. The equivalent FOSLS formulation from [10] minimizes the least-squares functional

$$LS(f; v, q) := \|q - \nabla v\|_{L^2(\Omega)}^2 + \|f + \omega^2 v + \operatorname{div} q\|_{L^2(\Omega)}^2$$

over all $(v, q) \in X$ with norm as in subsection 2.1.

2.3. Linear elasticity. Given $f \in L^2(\Omega; \mathbb{R}^d)$, the linear elasticity seeks the solution $(u, \sigma) \in X := H_0^1(\Omega; \mathbb{R}^d) \times H(\operatorname{div}, \Omega; \mathbb{R}^{d \times d})$ to

$$-\operatorname{div} \sigma = f \quad \text{and} \quad \sigma = \mathbb{C}\varepsilon(u)$$

with the linear Green strain tensor $\varepsilon(u) := (\nabla u + (\nabla u)^\top)/2$, positive Lamé constants λ and μ , and the fourth-order elasticity tensor \mathbb{C} [14]. The problem is equivalent to the minimization of the least-squares functional

$$LS(f; v, \tau) := \|\mathbb{C}^{-1/2}\tau - \mathbb{C}^{1/2}\varepsilon(v)\|_{L^2(\Omega)}^2 + \|f + \operatorname{div} \tau\|_{L^2(\Omega)}^2$$

over all $(v, \tau) \in X$ with norm $\|(v, \tau)\|_X^2 := \|\mathbb{C}^{1/2}\varepsilon(v)\|_{L^2(\Omega)}^2 + \|\mathbb{C}^{-1/2}\tau\|_{L^2(\Omega)}^2 + \|\operatorname{div} \tau\|_{L^2(\Omega)}^2$ [9].

2.4. Time-harmonic Maxwell equations. Given some right-hand side $f \in L^2(\Omega; \mathbb{R}^3)$ and a frequency $\omega^2 > 0$ different from an eigenvalue of the resonant cavity problem, the time-harmonic Maxwell equations in $d = 3$ space dimensions seek $(E, H) \in X := H_0(\text{curl}, \Omega) \times H(\text{curl}, \Omega)$ with

$$-\omega^2 E + \text{curl} H = f \text{ in } \Omega \quad \text{and} \quad \text{curl} E - H = 0 \text{ in } \Omega.$$

The problem is well posed and its solution minimizes the least-squares functional

$$LS(f; F, G) := \|G - \text{curl} F\|_{L^2(\Omega)}^2 + \|f + \omega^2 F - \text{curl} G\|_{L^2(\Omega)}^2$$

over all $(F, G) \in X$ with norm $\|(F, G)\|_X^2 := \omega^4 \|F\|_{L^2(\Omega)}^2 + \|\text{curl} F\|_{L^2(\Omega)}^2 + \|G\|_{L^2(\Omega)}^2 + \|\text{curl} G\|_{L^2(\Omega)}^2$. This problem is related to the problem in [6] with the exception of an additional term similar to the extra term in subsection 3.3.

2.5. Discretization. Let \mathbb{T} be the set of admissible and shape regular triangulations of the polyhedral bounded Lipschitz domain $\Omega \subset \mathbb{R}^d$ into simplices [5, Chap. 5]. Given $\delta > 0$, the subset $\mathbb{T}(\delta) \subset \mathbb{T}$ consists of all triangulations $\mathcal{T} \in \mathbb{T}$ with diameter $h_T := \text{diam}(T) < \delta$ for all $T \in \mathcal{T}$. Let $\mathbb{P}_k(T; \mathbb{R}^\ell)$ denote the set of polynomials of total degree at most $k \in \mathbb{N}_0$ seen as a map from T to \mathbb{R}^ℓ , $\ell \in \mathbb{N}$, and define $RT_k(T) := \mathbb{P}_k(T; \mathbb{R}^\ell) + \mathbb{P}_k(T; \mathbb{R}) \text{id} \subset \mathbb{P}_k(T; \mathbb{R}^\ell)$ and $\mathcal{N}^k(T) := \mathbb{P}_k(T; \mathbb{R}^3) + \mathbb{P}_k(T; \mathbb{R}^3) \times \text{id} \subset \mathbb{P}_k(T; \mathbb{R}^3)$ with the identity id on T . Define for all $k \in \mathbb{N}_0$ the Courant, Raviart–Thomas, and Nédélec element spaces

$$\begin{aligned} S^{k+1}(\mathcal{T}) &:= \{V \in H^1(\Omega) : \forall T \in \mathcal{T}, V|_T \in \mathbb{P}_{k+1}(T; \mathbb{R})\}, \\ RT_k(\mathcal{T}) &:= \{Q \in H(\text{div}, \Omega) : \forall T \in \mathcal{T}, Q|_T \in RT_k(T)\}, \\ \mathcal{N}^k(\mathcal{T}) &:= \{F \in H(\text{curl}, \Omega) : \forall T \in \mathcal{T}, F|_T \in \mathcal{N}^k(T)\}. \end{aligned}$$

Furthermore, set $S_0^{k+1}(\mathcal{T}) := S^{k+1}(\mathcal{T}) \cap H_0^1(\Omega)$ and $\mathcal{N}_0^k(\mathcal{T}) := \mathcal{N}^k(\mathcal{T}) \cap H_0(\text{curl}, \Omega)$. It is well known and understood throughout this paper that the discrete spaces $X(\mathcal{T})$ in Table 2 and the continuous spaces X satisfy the pointwise density property [4, 5, 7]

$$(D) \quad \forall \varepsilon > 0 \quad \forall w \in X \quad \exists \delta > 0 \quad \forall \mathcal{T} \in \mathbb{T}(\delta) \quad \exists W \in X(\mathcal{T}) \quad \|w - W\|_X < \varepsilon.$$

3. Proof of the asymptotic exactness. The unifying analysis departs with an abstract framework and thereafter applies it to the model examples of section 2.

3.1. An abstract setting. This subsection provides an abstract asymptotic exactness result based on three hypotheses.

(H1) Suppose $a : X \times X \rightarrow \mathbb{R}$ is a scalar product that is equivalent to the scalar product b on the real Hilbert space (X, b) with associated norm $\|\bullet\|_b = \|\bullet\|_X$. In particular, there exist positive constants α, β with

$$(2) \quad \forall x \in X \quad \alpha \|x\|_b^2 \leq a(x, x) =: \|x\|_a^2 \leq \beta \|x\|_b^2.$$

(H2) Suppose that there exist countably many pairwise distinct positive numbers $\mu(0) = 1, \mu(1), \mu(2), \mu(3), \dots$ with closed eigenspaces $E(\mu(j)) \subset X$ for $j \in \mathbb{N}_0$ and

$$(3) \quad \forall j \in \mathbb{N}_0 \quad \forall \phi_j \in E(\mu(j)) \quad \forall x \in X \quad a(\phi_j, x) = \mu(j)b(\phi_j, x).$$

Let the eigenspaces have finite dimension $\dim E(\mu(j)) \in \mathbb{N}$ for all $j \in \mathbb{N}$ (while $\dim E(\mu(0)) \in \mathbb{N}_0 \cup \{\infty\}$ may be infinity or zero), and suppose that the linear hull of all eigenspaces $E(\mu(0)), E(\mu(1)), \dots$ is dense in X ,

$$(4) \quad X = \overline{\text{span}\{E(\mu(j)) : j \in \mathbb{N}_0\}}.$$

(H3) Suppose $\mu(0) = 1$ is the only accumulation point of $(\mu(j))_{j \in \mathbb{N}_0}$, $\lim_{j \rightarrow \infty} \mu(j) = 1$.

Given a right-hand side $F \in X^*$ in the dual X^* of X , let $u \in X$ be the unique solution to $a(u, v) = F(v)$ for all $v \in X$. Furthermore, let $X(\mathcal{T}) \subset X$ satisfy the density property **(D)**, and define the discrete solution $U \in X(\mathcal{T})$ with $a(U, V) = F(V)$ for all $V \in X(\mathcal{T})$.

THEOREM 3.1. *Suppose **(H1)**–**(H3)**, **(D)**, and $\varepsilon > 0$. Then there exists some $\delta > 0$ for all $F \in X^*$ such that for all $\mathcal{T} \in \mathbb{T}(\delta)$*

$$(5) \quad (1 - \varepsilon)\|u - U\|_b^2 \leq \|u - U\|_a^2 \leq (1 + \varepsilon)\|u - U\|_b^2.$$

Some remarks are in order before the proof of the theorem concludes this subsection.

Remark 3.2 (bounded eigenvalues). It follows from **(H1)** that $\mu(0), \mu(1), \mu(2), \dots$ are bounded in the compact interval $[\alpha, \beta]$ and, since $\mu(0) = 1$, it holds that $\alpha \leq 1 \leq \beta$.

Remark 3.3 (orthogonal eigenspaces). The eigenvectors $\phi_j \in E(\mu(j))$ and $\phi_k \in E(\mu(k))$ with $j, k \in \mathbb{N}$ satisfy $\mu(j)b(\phi_j, \phi_k) = a(\phi_j, \phi_k) = a(\phi_k, \phi_j) = \mu(k)b(\phi_k, \phi_j)$. If $j \neq k$, it holds that $0 \neq \mu(j) \neq \mu(k) \neq 0$, and so $b(\phi_j, \phi_k) = a(\phi_j, \phi_k) = 0$. Thus,

$$(6) \quad \forall j, k \in \mathbb{N}_0 \wedge j \neq k \quad E(\mu(j)) \perp_a E(\mu(k)) \text{ and } E(\mu(j)) \perp_b E(\mu(k)).$$

Remark 3.4 (orthogonal decomposition of X). Given an index set $J \subset \mathbb{N}_0$, define $X(J)$ as the closure of $\text{span}\{E(\mu(j)) : j \in J\}$, and set the complement $J^c := \mathbb{N}_0 \setminus J$. Then (4) implies that any $v \in X$ can be decomposed into $v = w + z$ with some $w = \sum_{j \in J} w_j \in X(J)$ and some $z = \sum_{k \in J^c} z_k \in X(J^c)$ such that $w_j \in E(\mu(j))$ for all $j \in J$ and $z_k \in E(\mu(k))$ for all $k \in J^c$. Since $X(J)$ and $X(J^c)$ are closed with respect to the norm $\|\bullet\|_b$, (6) implies $b(w, z) = 0$. This proves the b -orthogonality $X(J) \perp_b X(J^c)$. Similar arguments and the equivalence (2) of $\|\bullet\|_b$ and $\|\bullet\|_a$ imply the a -orthogonality $X(J) \perp_a X(J^c)$.

Remark 3.5 (built-in error control of LSFEMs). The least-squares formulations from section 2 allow **(H1)**–**(H3)** such that $\|u - U\|_a^2 = LS(f; U)$ is a computable residual and serves as an error estimator for the unknown error $\|u - U\|_b = \|u - U\|_X$. The ellipticity in **(H1)** leads to

$$(7) \quad \alpha\|u - U\|_b^2 \leq LS(f; U) = \|u - U\|_a^2 \leq \beta\|u - U\|_b^2.$$

This is well known in the least-squares community and called reliability and efficiency in the a posteriori error analysis. It is a consequence of Theorem 3.1 that the GUB in (7) leads to an overestimation by the factor α^{-1} as the mesh size tends to zero.

Proof of Theorem 3.1. The Galerkin orthogonality $a(u - U, W) = 0$ for all $W \in X(\mathcal{T})$ is rewritten as $u - U \in X(\mathcal{T})^\perp := \{v \in X : \forall W \in X(\mathcal{T}), a(v, W) = 0\}$. Then the theorem follows from the more general assertion

$$(8) \quad \forall \varepsilon > 0 \exists \delta > 0 \forall \mathcal{T} \in \mathbb{T}(\delta) \forall v \in X(\mathcal{T})^\perp \quad (1 - \varepsilon)\|v\|_b^2 \leq \|v\|_a^2 \leq (1 + \varepsilon)\|v\|_b^2.$$

To prove (8), let $0 < \varepsilon < 1$ and $v \in X(\mathcal{T})^\perp$ with $\|v\|_b = 1$.

Step 1 (decomposition of v). Recall $\mu(0), \mu(1), \dots$ from **(H2)**, and, given $\varepsilon > 0$, define the index set $J(\varepsilon) := \{j \in \mathbb{N} : |1 - \mu(j)| > \varepsilon\}$ with complement $J^c(\varepsilon) := \mathbb{N}_0 \setminus J(\varepsilon)$. It is a consequence of **(H3)** that the index set $J(\varepsilon)$ is finite. As outlined

TABLE 2
Notation in subsection 3.2.

	\mathbb{M}	A	γ	D	D^*	$X(\mathcal{T})$
Poisson	\mathbb{R}^d	id	0	∇	$-\text{div}$	$S_0^{k+1}(\mathcal{T}) \times RT_k(\mathcal{T})$
Helmholtz	\mathbb{R}^d	id	ω^2	∇	$-\text{div}$	$S_0^{k+1}(\mathcal{T}) \times RT_k(\mathcal{T})$
Elasticity	$\mathbb{R}^{d \times d}$	\mathbb{C}	0	$\varepsilon(\bullet)$	$-\text{div}$	$S_0^{k+1}(\mathcal{T})^d \times RT_k(\mathcal{T})^d$
Maxwell	\mathbb{R}^3	id	ω^2	curl	curl	$\mathcal{N}_0^k(\mathcal{T}) \times \mathcal{N}^k(\mathcal{T})$

in Remark 3.4, **(H2)** leads to the a - and b -orthogonal decomposition $v = w + z$ with $w \in X(J(\varepsilon))$ and $z \in X(J^c(\varepsilon))$. The Pythagoras theorem reads

$$(9) \quad 1 = \|v\|_b^2 = \|w\|_b^2 + \|z\|_b^2 \quad \text{and} \quad \|v\|_a^2 = \|w\|_a^2 + \|z\|_a^2.$$

Step 2 (upper bound for $\|w\|_a$). Let (ϕ_1, \dots, ϕ_m) be a b -orthonormal basis of $\text{span}\{E(\mu(j)) : j \in J(\varepsilon)\} = \text{span}\{\phi_1, \dots, \phi_m\}$ with $w = \sum_{k=1}^m \xi_k \phi_k$. The density **(D)** leads to $\delta > 0$ such that for all $k = 1, \dots, m$ and $\mathcal{T} \in \mathbb{T}(\delta)$ there exists a $\Phi_k \in X(\mathcal{T})$ with $\|\phi_k - \Phi_k\|_b \leq \varepsilon/\sqrt{m}$. The discrete $W := \sum_{k=1}^m \xi_k \Phi_k \in X(\mathcal{T})$ satisfies

$$\|w - W\|_b \leq \sum_{k=1}^m |\xi_k| \|\phi_k - \Phi_k\|_b \leq m^{-1/2} \varepsilon \sum_{k=1}^m |\xi_k| \leq \varepsilon \left(\sum_{k=1}^m \xi_k^2 \right)^{1/2} = \varepsilon \|w\|_b.$$

The combination with $a(w, z) = 0 = a(v, W)$, a Cauchy–Schwarz inequality, and (2) proves

$$(10) \quad \|w\|_a^2 = a(w, v) = a(w - W, v) \leq \beta \|w - W\|_b \leq \varepsilon \beta \|w\|_b \leq \alpha^{-1/2} \varepsilon \beta \|w\|_a.$$

Step 3 (upper and lower bounds for $\|z\|_a^2$). Since z is in the closure of the linear hull $\text{span}\{E(\mu(j)) : j \in J^c(\varepsilon)\}$ with respect to $\|\bullet\|_a$ and $\|\bullet\|_b$, the sums $\|z\|_a^2 = \sum_{j \in J^c(\varepsilon)} \|z_j\|_a^2$ and $\|z\|_b^2 = \sum_{j \in J^c(\varepsilon)} \|z_j\|_b^2$ converge. Then $1 - \varepsilon \leq \mu(j) \leq 1 + \varepsilon$ and $\|z_j\|_a^2 = \mu(j) \|z_j\|_b^2$ for all $j \in J^c(\varepsilon)$ imply

$$(11) \quad (1 - \varepsilon) \|z\|_b^2 \leq \|z\|_a^2 \leq (1 + \varepsilon) \|z\|_b^2.$$

Step 4 (upper bound for $\|v\|_a^2$). The combination of (9)–(11) proves

$$\|v\|_a^2 = \|z\|_a^2 + \|w\|_a^2 \leq (1 + \varepsilon) \|z\|_b^2 + \|w\|_a^2 \leq 1 + \varepsilon + \varepsilon^2 \beta^2 / \alpha.$$

Step 5 (lower bound for $\|v\|_a^2$). The combination of (2) and (9)–(10) shows $1 - \varepsilon^2 \beta^2 / \alpha^2 \leq 1 - \|w\|_a^2 / \alpha \leq 1 - \|w\|_b^2 = \|z\|_b^2$. Consequently,

$$(1 - \varepsilon)(1 - \varepsilon^2 \beta^2 / \alpha^2) \leq (1 - \varepsilon) \|z\|_b^2 \leq \|z\|_a^2 \leq \|w\|_a^2 + \|z\|_a^2 = \|v\|_a^2.$$

Relabeling ε and δ for sufficiently small ε concludes the proof of (8). \square

3.2. A class of problems sufficient for **(H1)–**(H3)**.** This subsection compiles the model problems in section 2 and verifies the assumptions of Theorem 3.1. Table 2 displays the particular meanings of the following abstract operators.

For all examples of section 2 the positive definite isomorphism $A = A^{1/2} \circ A^{1/2}$ maps the subspace $\mathbb{M} \subset \mathbb{R}^{m \times n}$ with $m, n \in \mathbb{N}$ onto \mathbb{M} . Furthermore, the linear differential operator D maps the real Hilbert space V with norm $\|\bullet\|_V^2 = \|\bullet\|_{L^2(\Omega)}^2 + \|A^{1/2} D \bullet\|_{L^2(\Omega)}^2$ onto a closed subset of $L^2(\Omega; \mathbb{M})$. Since $D : V \rightarrow L^2(\Omega; \mathbb{M})$ is bounded, its kernel $\ker D$ is closed. This leads to the existence of an orthogonal complement

$W \subset V$ with $W \perp_V \ker D$ and $V = W \oplus \ker D$. There exist countably many eigenpairs $(\lambda_j, \psi_j) \in \mathbb{R} \times W \setminus \{0\}$ with $D^*AD\psi_j = \lambda_j\psi_j$ for $j \in \mathbb{N}$, i.e.,

$$(12) \quad \forall v \in V \quad (AD\psi_j, Dv)_{L^2(\Omega)} = \lambda_j(\psi_j, v)_{L^2(\Omega)}.$$

Moreover, $0 < \lambda_1 \leq \lambda_2 \leq \dots$ with $\lim_{j \rightarrow \infty} \lambda_j = \infty$. The eigenfunctions $(\psi_j)_{j \in \mathbb{N}}$ form a basis of $W = \overline{\text{span}\{\psi_j : j \in \mathbb{N}\}}$ in V and are orthonormal in the sense that $(\psi_j, \psi_k)_{L^2(\Omega)} = \delta_{jk}$ and $(AD\psi_j, D\psi_k)_{L^2(\Omega)} = \lambda_j\delta_{jk}$ for all $j, k \in \mathbb{N}$.

Remark 3.6. In the Poisson model problem and the Helmholtz equation (resp., linear elasticity and Maxwell equations), $\lambda_1, \lambda_2, \dots$ are the Dirichlet eigenvalues of the Laplace operator (resp., the Dirichlet eigenvalues of the Lamé operator and the eigenvalues of the resonant cavity problem). It is known that the eigenfunctions of (12) satisfy the aforementioned properties [4, p. 15], [15, p. 720], [19, p. 97].

Define for any $\tau \in L^2(\Omega; \mathbb{M})$ and $\chi \in L^2(\Omega; \mathbb{R}^m)$ with $(\tau, Dv)_{L^2(\Omega)} = (\chi, v)_{L^2(\Omega)}$ for all $v \in V$ the operator $D^*\tau := \chi$, and set

$$\Sigma := \{\tau \in L^2(\Omega; \mathbb{M}) : D^*\tau \in L^2(\Omega; \mathbb{R}^m)\}, \quad \|\bullet\|_{\Sigma}^2 := \|A^{-1/2}\bullet\|_{L^2(\Omega)}^2 + \|D^*\bullet\|_{L^2(\Omega)}^2.$$

In all model problems $(\Sigma, \|\bullet\|_{\Sigma})$ is a Hilbert space [4]. Since $D^* : \Sigma \rightarrow L^2(\Omega; \mathbb{R}^m)$ is linear and bounded, the kernel $\ker D^*$ is a closed subspace of Σ . Theorem 3.7 and Lemma 3.9 are well known in the least-squares community but are stated for completeness.

THEOREM 3.7 (equivalence of primal and first-order problem). *Given a right-hand side $f \in L^2(\Omega; \mathbb{R}^m)$ and a constant $\gamma \in \mathbb{R}$, $u \in V$ solves the primal problem*

$$(13) \quad \forall v \in V \quad (ADu, Dv)_{L^2(\Omega)} - \gamma(u, v)_{L^2(\Omega)} = (f, v)_{L^2(\Omega)}$$

if and only if $(u, \sigma) = (u, ADu) \in V \times \Sigma$ is the unique minimizer amongst all $(v, \tau) \in X := V \times \Sigma$ of the least-squares functional

$$LS(f; v, \tau) := \|A^{-1/2}\tau - A^{1/2}Dv\|_{L^2(\Omega)}^2 + \|f + \gamma v - D^*\tau\|_{L^2(\Omega)}^2.$$

Proof. The solution $u \in V$ to the primal problem (13) satisfies $(ADu, Dw)_{L^2(\Omega)} = (f + \gamma u, w)_{L^2(\Omega)}$ for all $w \in V$. This shows $ADu \in \Sigma$ with $D^*ADu = f + \gamma u \in L^2(\Omega; \mathbb{R}^m)$ and proves $LS(f; u, ADu) = 0$. On the other hand, any $(v, \tau) \in X$ with $LS(f; v, \tau) = 0$ satisfies $\tau = ADv$ and so $D^*ADv - \gamma v = f$. Consequently $v \in V$ solves (13). The uniqueness of the solution implies $v = u$. \square

Throughout this paper, (13) is well posed because either the kernel $\ker D = \{0\}$ is trivial and $\gamma = 0$ or $\gamma \in (0, \infty) \setminus \{\lambda_1, \lambda_2, \dots\}$. Theorem 3.7 guarantees the equivalence of (13) and the minimization of $LS(f; \bullet)$ over all $(v, \tau) \in X := V \times \Sigma$ with norm $\|(v, \tau)\|_X = \|(v, \tau)\|_b$ induced by

$$\begin{aligned} b(u, \sigma; v, \tau) &= \gamma^2(u, v)_{L^2(\Omega)} + (A^{1/2}Du, A^{1/2}Dv)_{L^2(\Omega)} \\ &\quad + (A^{-1/2}\sigma, A^{-1/2}\tau)_{L^2(\Omega)} + (D^*\sigma, D^*\tau)_{L^2(\Omega)}. \end{aligned}$$

The minimizer $(u, \sigma) \in X$ of the least-squares functional is characterized as the solution to $a(u, \sigma; v, \tau) = -(f, \gamma v - D^*\tau)_{L^2(\Omega)}$ for all $(v, \tau) \in X$ with the symmetric bilinear form

$$\begin{aligned} a(u, \sigma; v, \tau) &:= (A^{1/2}Du - A^{-1/2}\sigma, A^{1/2}Dv - A^{-1/2}\tau)_{L^2(\Omega)} \\ &\quad + (\gamma u - D^*\sigma, \gamma v - D^*\tau)_{L^2(\Omega)}. \end{aligned}$$

Remark 3.8. Since most of the results in this work follow from a spectral analysis, the scalar products read $a(\bullet, \bullet)$ and $b(\bullet, \bullet)$ rather than $\langle L\bullet, L\bullet \rangle_0 := a(\bullet, \bullet)$ and $\langle \bullet, \bullet \rangle_X := b(\bullet, \bullet)$, which is more frequent in least-squares publications.

LEMMA 3.9. *The following splits are orthogonal with respect to $(A^{-1}\bullet, \bullet)_{L^2(\Omega)}$:*

$$(14) \quad L^2(\Omega; \mathbb{M}) = AD(V) \oplus \ker D^* \quad \text{and} \quad \Sigma = (AD(V) \cap \Sigma) \oplus \ker D^*.$$

Proof. Step 1 (decomposition of $L^2(\Omega; \mathbb{M})$). Since the norm $\|A^{1/2}D\bullet\|_{L^2(\Omega)}$ in W is equivalent to $\|\bullet\|_V$, $(W, (AD\bullet, D\bullet)_{L^2(\Omega)})$ is a Hilbert space. Given any $\sigma \in L^2(\Omega; \mathbb{M})$, the Riesz representation $\xi \in W$ satisfies

$$\forall w \in W \quad (AD\xi, Dw)_{L^2(\Omega)} = (\sigma, Dw)_{L^2(\Omega)}.$$

Define $\sigma_0 := \sigma - AD\xi$ with $(\sigma_0, Dw)_{L^2(\Omega)} = (\sigma, Dw)_{L^2(\Omega)} - (AD\xi, Dw)_{L^2(\Omega)} = 0$ for all $w \in W$, whence $\sigma_0 \in \ker D^*$. Since $\sigma_0 \in \ker D^*$ and $(A^{-1}ADv, \sigma_0)_{L^2(\Omega)} = (v, D^*\sigma_0)_{L^2(\Omega)} = 0$ for all $v \in V$, the split is orthogonal.

Step 2 (decomposition of Σ). Given $\sigma \in \Sigma$, the split in $L^2(\Omega; \mathbb{M})$ leads to $\xi \in V$ and $\sigma_0 \in \ker D^* \subset \Sigma$ with $\sigma = AD\xi + \sigma_0$ and $(A^{-1}AD\xi, \sigma_0)_{L^2(\Omega)} = 0$. Since $\sigma, \sigma_0 \in \Sigma$ and Σ is a vector space, $AD\xi = \sigma - \sigma_0 \in \Sigma$. \square

Remark 3.6 and (12) imply for each model problem in section 2 that the subspace $\text{span}\{AD\psi_j : j \in \mathbb{N}\} \subset \Sigma$ is dense in $AD(V) \cap \Sigma$ with respect to $\|\bullet\|_\Sigma$, i.e., $AD(V) \cap \Sigma = \text{span}\{AD\psi_j : j \in \mathbb{N}\}$. For all $j \in \mathbb{N}$ define $\nu_j := \lambda_j(\gamma + 1)^2 / ((\lambda_j + 1)(\gamma^2 + \lambda_j))$ and set $\mu_0 := 1$ and $\phi_0 \in \ker D \times \ker D^* \subset X$,

$$(15a) \quad \mu_{2j-1} := 1 - \nu_j^{1/2} \quad \text{and} \quad \phi_{2j-1} := \left((\lambda_j^2 + \lambda_j)^{1/2} (\gamma^2 + \lambda_j)^{-1/2} \psi_j, AD\psi_j \right) \in X,$$

$$(15b) \quad \mu_{2j} := 1 + \nu_j^{1/2} \quad \text{and} \quad \phi_{2j} := \left((\lambda_j^2 + \lambda_j)^{1/2} (\gamma^2 + \lambda_j)^{-1/2} \psi_j, -AD\psi_j \right) \in X.$$

THEOREM 3.10. *The formulae in (15) define the least-squares eigenpairs*

$$(16) \quad \forall j \in \mathbb{N}_0 \quad \forall (v, \tau) \in X \quad a(\phi_j; v, \tau) = \mu_j b(\phi_j; v, \tau).$$

Proof. Step 1 (decomposition of the bilinear forms). Given $(u, \sigma), (v, \tau) \in X$, (14) leads to $\xi, \vartheta \in W$ and $\sigma_0, \tau_0 \in \ker D^*$ with $AD\xi, AD\vartheta \in \Sigma$, $\sigma = AD\xi + \sigma_0$, and $\tau = AD\vartheta + \tau_0$. Furthermore, $W = \overline{\text{span}\{\psi_j : j \in \mathbb{N}\}}$ and $V = W \oplus \ker D$ show the existence of coefficients $u_j, v_j, \xi_j, \vartheta_j \in \mathbb{R}$ for $j \in \mathbb{N}$ and elements $u_0, v_0 \in \ker D$ with

$$u = u_0 + \sum_{j \in \mathbb{N}} u_j \psi_j, \quad v = v_0 + \sum_{j \in \mathbb{N}} v_j \psi_j, \quad \xi = \sum_{j \in \mathbb{N}} \xi_j \psi_j, \quad \text{and} \quad \vartheta = \sum_{j \in \mathbb{N}} \vartheta_j \psi_j.$$

The density of $\text{span}\{\psi_j : j \in \mathbb{N}\}$ in $W \subset V$, the density of $\text{span}\{AD\psi_j : j \in \mathbb{N}\}$ in

$AD(V) \cap \Sigma \subset \Sigma$, and the orthogonality of the eigenfunctions imply

$$\begin{aligned} a(u, \sigma; v, \tau) &= (A^{1/2}D(u - \xi) - A^{-1/2}\sigma_0, A^{1/2}D(v - \vartheta) - A^{-1/2}\tau_0)_{L^2(\Omega)} \\ &\quad + (\gamma u - D^*AD\xi, \gamma v - D^*AD\vartheta)_{L^2(\Omega)} \\ &= \left(\sum_{j \in \mathbb{N}} (u_j - \xi_j) A^{1/2}D\psi_j, \sum_{k \in \mathbb{N}} (v_k - \vartheta_k) A^{1/2}D\psi_k \right)_{L^2(\Omega)} \\ &\quad + \left(\sum_{j \in \mathbb{N}} (\gamma u_j - \lambda_j \xi_j) \psi_j, \sum_{k \in \mathbb{N}} (\gamma v_k - \lambda_k \vartheta_k) \psi_k \right)_{L^2(\Omega)} \\ &\quad + (A^{-1/2}\sigma_0, A^{-1/2}\tau_0)_{L^2(\Omega)} + \gamma^2(u_0, v_0)_{L^2(\Omega)} \\ &= \sum_{j \in \mathbb{N}} \begin{pmatrix} u_j \\ \xi_j \end{pmatrix} \cdot \begin{pmatrix} \lambda_j + \gamma^2 & -\lambda_j - \gamma\lambda_j \\ -\lambda_j - \gamma\lambda_j & \lambda_j + \lambda_j^2 \end{pmatrix} \begin{pmatrix} v_j \\ \vartheta_j \end{pmatrix} \\ &\quad + (A^{-1/2}\sigma_0, A^{-1/2}\tau_0)_{L^2(\Omega)} + \gamma^2(u_0, v_0)_{L^2(\Omega)}. \end{aligned}$$

Similar arguments lead to

$$\begin{aligned} b(u, \sigma; v, \tau) &= \sum_{j \in \mathbb{N}} \begin{pmatrix} u_j \\ \xi_j \end{pmatrix} \cdot \begin{pmatrix} \lambda_j + \gamma^2 & 0 \\ 0 & \lambda_j + \lambda_j^2 \end{pmatrix} \begin{pmatrix} v_j \\ \vartheta_j \end{pmatrix} \\ &\quad + (A^{-1/2}\sigma_0, A^{-1/2}\tau_0)_{L^2(\Omega)} + \gamma^2(u_0, v_0)_{L^2(\Omega)}. \end{aligned}$$

Step 2 (computation of eigenpairs). The decomposition of a and b in Step 1 shows that $\mu_0 = 1$ satisfies (16) for all elements ϕ_0 in $\ker D \times \ker D^*$. Moreover, the decomposition leads for all $j \in \mathbb{N}$ and all $(v, \tau) \in X$ with decomposition as in Step 1 to

$$\begin{aligned} a(\phi_{2j-1}; v, \tau) &= \begin{pmatrix} (\lambda_j^2 + \lambda_j)^{1/2}(\gamma^2 + \lambda_j)^{-1/2} \\ 1 \end{pmatrix} \cdot \begin{pmatrix} \lambda_j + \gamma^2 & -\lambda_j - \gamma\lambda_j \\ -\lambda_j - \gamma\lambda_j & \lambda_j + \lambda_j^2 \end{pmatrix} \begin{pmatrix} v_j \\ \vartheta_j \end{pmatrix} \\ &= \mu_{2j-1} \begin{pmatrix} (\lambda_j^2 + \lambda_j)^{1/2}(\gamma^2 + \lambda_j)^{-1/2} \\ 1 \end{pmatrix} \cdot \begin{pmatrix} \lambda_j + \gamma^2 & 0 \\ 0 & \lambda_j + \lambda_j^2 \end{pmatrix} \begin{pmatrix} v_j \\ \vartheta_j \end{pmatrix} \\ &= \mu_{2j-1} b(\phi_{2j-1}; v, \tau). \end{aligned}$$

Analogously, $a(\phi_{2j}; v, \tau) = \mu_{2j} b(\phi_{2j}; v, \tau)$ follows for all $j \in \mathbb{N}$ and $(v, \tau) \in X$. □

THEOREM 3.11. *The model problems satisfy (H1)–(H3) and (1).*

Proof. Step 1 (proof of (3) from (H2)). The countably many numbers μ_0, μ_1, \dots from (15) lead to countably many pairwise distinct numbers $\mu(0) = 1, \mu(1), \mu(2), \dots$ with $\{\mu_k : k \in \mathbb{N}_0\} = \{\mu(j) : j \in \mathbb{N}_0\}$. Theorem 3.10 (resp., Theorem SM1.1) proves that the closed subspaces $E(\mu(0)) := \ker D \times \ker D^*$ and $E(\mu(j)) := \text{span}\{\phi_k : k \in \mathbb{N}, \mu_k = \mu(j)\}$ for all $j \in \mathbb{N}$ with ϕ_k from (15) (resp., (SM2)) satisfy (3).

Step 2 (proof of (H3)). It follows from a simple calculation that μ_{2j-1} and μ_{2j} from (15) (resp., (SM1)), and so $\mu(j)$ tend to one as j (and so λ_j) tends to infinity.

Step 3 (proof of $\dim E(\mu(j)) \in \mathbb{N}$ for all $j \in \mathbb{N}$ from (H2)). The eigenspace $E(\mu(j))$ is the span of ϕ_k with $\mu_k = \mu(j)$. Since the eigenfunctions ϕ_1, ϕ_2, \dots are linearly independent, it holds with the counting measure $|\bullet|$ that

$$(17) \quad \dim E(\mu(j)) = |\{k \in \mathbb{N} : \mu_k = \mu(j)\}|.$$

It follows from $\lim_{k \rightarrow \infty} \mu_k = 1$ and $\mu(j) \neq 1$ that (17) is for all $j \in \mathbb{N}$ a finite number.

TABLE 3

Eigenvalues μ_j with (16) (resp., (18)) as a function of the eigenvalues λ_j with (12) for all $j \in \mathbb{N}$.

Problem	Least-squares eigenvalues
Poisson Elasticity	$\mu_{2j-1} = 1 - (\lambda_j + 1)^{-1/2}$ $\mu_{2j} = 1 + (\lambda_j + 1)^{-1/2}$
Helmholtz	$\mu_{2j-1} = \frac{\omega^4 + 2\lambda_j}{2\lambda_j} - \sqrt{\frac{(\omega^4 + 2\lambda_j)^2}{4\lambda_j^2} - \frac{(\omega^2 - \lambda_j)^2}{(\lambda_j + 1)\lambda_j}}$ $\mu_{2j} = \frac{\omega^4 + 2\lambda_j}{2\lambda_j} + \sqrt{\frac{(\omega^4 + 2\lambda_j)^2}{4\lambda_j^2} - \frac{(\omega^2 - \lambda_j)^2}{(\lambda_j + 1)\lambda_j}}$
Maxwell	$\mu_{2j-1} = 1 - (1 - (\omega^2 - \lambda_j)^2(\lambda_j + 1)^{-1}(\omega^4 + \lambda_j)^{-1})^{1/2}$ $\mu_{2j} = 1 - (1 + (\omega^2 - \lambda_j)^2(\lambda_j + 1)^{-1}(\omega^4 + \lambda_j)^{-1})^{1/2}$

*Step 4 (proof of $X = \overline{\text{span}\{E(\mu(j)) : j \in \mathbb{N}_0\}}$ from **(H2)**).* The model problems satisfy either $\gamma \neq 0$ or $\gamma = 0$ and $\ker D = \{0\}$. If $\gamma \neq 0$, it holds for all $(v, \tau) \in \Sigma$ that

$$\min\{1, \gamma^2\}(\|v\|_V^2 + \|\tau\|_\Sigma^2) \leq \|(v, \tau)\|_b^2 \leq \max\{1, \gamma^2\}(\|v\|_V^2 + \|\tau\|_\Sigma^2),$$

and with $\ker D = \{0\}$ it holds that $(1 + \gamma^2\lambda_1^{-1})^{-1}\|(v, \tau)\|_b \leq \|(v, \tau)\|_{b_0} \leq \|(v, \tau)\|_b$. If $\ker D = \{0\}$ and $\gamma = 0$, it holds for all $(v, \tau) \in \Sigma$ that

$$(1 + \lambda_1^{-1})^{-1}(\|v\|_V^2 + \|\tau\|_\Sigma^2) \leq \|(v, \tau)\|_b^2 \leq \|v\|_V^2 + \|\tau\|_\Sigma^2.$$

Hence, the norms $\|\bullet\|_b$ and $\|\bullet\|_{V \times \Sigma} := (\|\bullet\|_V^2 + \|\bullet\|_\Sigma^2)^{1/2}$ (resp., $\|\bullet\|_{b_0}$ and $\|\bullet\|_{V \times \Sigma}$) are equivalent. Since $W = \text{span}\{\psi_j : j \in \mathbb{N}\}$ in V , $(\psi_j, 0) \in \text{span}\{E(\mu(k)) : k \in \mathbb{N}\}$ for all $j \in \mathbb{N}$, and $\ker D \subset E(\mu(0))$, the equivalence of the norms and $V = W \oplus \ker D$ lead to

$$V \times \{0\} \subset \ker D \times \{0\} \oplus \overline{\text{span}\{(\psi_j, 0) : j \in \mathbb{N}\}} \subset \overline{\text{span}\{E(\mu(j)) : j \in \mathbb{N}\}}.$$

The density of $\text{span}\{AD\psi_1, AD\psi_2, \dots\}$ in $AD(V) \cap \Sigma$ implies that $(0, AD\psi_j) \in \text{span}\{E(\mu(k)) : k \in \mathbb{N}\}$ for all $j \in \mathbb{N}$. With the equivalence of the norms this leads to

$$\{0\} \times \Sigma \subset \{0\} \times \ker D^* \oplus \overline{\text{span}\{(0, AD\psi_j) : j \in \mathbb{N}\}} \subset \overline{\text{span}\{E(\mu(j)) : j \in \mathbb{N}\}}.$$

*Step 5 (proof of **(H1)**).* The density of $\text{span}\{E(\mu(j)) : j \in \mathbb{N}_0\}$ in X proves

$$\inf_{j \in \mathbb{N}_0} \mu(j)\|(v, \tau)\|_b^2 \leq \|(v, \tau)\|_a^2 \leq \sup_{j \in \mathbb{N}_0} \mu(j)\|(v, \tau)\|_b^2$$

for any $(v, \tau) \in X$. Since $\gamma \notin \{\lambda_1, \lambda_2, \dots\}$ and $\lim_{j \rightarrow \infty} \mu(j) = 1$, this leads to (2) with $0 < \alpha := \min_{j \in \mathbb{N}_0} \mu(j) \leq \max_{j \in \mathbb{N}_0} \mu(j) =: \beta < \infty$.

Step 6 (proof of (1)). The application of Theorem 3.1 and $\|u - U\|_a^2 = LS(f; U)$ in the model problems results in (1). \square

Remark 3.12. It follows from $0 < \alpha := \min_{j \in \mathbb{N}_0} \mu(j) \leq \max_{j \in \mathbb{N}_0} \mu(j) =: \beta < \infty$ that $\alpha = \mu_1$ and $\beta = \mu_2$ with μ_1, μ_2 from Table 3 for the Poisson model problem and the linear elasticity. Furthermore, the Helmholtz equation and Maxwell equations satisfy $\alpha = \mu_{2j-1}$ and $\beta = \mu_{2j}$ for some $j \in \mathbb{N}$.

Remark 3.13. Table 3 shows that small eigenvalues λ of the differential operator D^*AD cause small and large eigenvalues μ in the Poisson model problem and the linear elasticity. However, small and large eigenvalues μ for the Maxwell and Helmholtz equations result not only from the size of the eigenvalues λ but also from the distance $|\lambda - \omega^2|$ to the frequency ω . Subsection 5.4 below presents a corresponding example with a huge preasymptotic regime caused by the necessity to resolve the high-frequency eigenfunctions sufficiently well.

Remark 3.14. The detailed analysis behind Table 3 is performed for four model problems but can be extended to other norms and bilinear forms exemplified for the alternative choice

$$b_0(u, \sigma; v, \tau) = (A^{1/2}Du, A^{1/2}Dv)_{L^2(\Omega)} + (A^{-1/2}\sigma, A^{-1/2}\tau)_{L^2(\Omega)} + (D^*\sigma, D^*\tau)_{L^2(\Omega)}$$

for all $(u, \sigma), (v, \tau) \in X$ for the Helmholtz equation in Table 3 and the ω -independent norm $\|\bullet\|_{b_0}$ induced by $b_0(\bullet, \bullet)$. The Helmholtz equation admits the eigenvalues $\mu_0 = 1$ and μ_j displayed for all $j \in \mathbb{N}$ in Table 3 of the eigenvalue problem

$$(18) \quad \forall (v, \tau) \in X \quad a(\phi_j; v, \tau) = \mu_j b_0(\phi_j; v, \tau).$$

This follows analogously from the proof of Theorem 3.10, and so details are provided in section SM1 of the supplementary material.

3.3. The Poisson model problem with H^1 -conforming compatible constraint. The following FOSLS method for the Poisson model problem [11, 13] is based on H^1 conforming ansatz functions and adds the constraint $\text{curl } p = 0$ to the problem in subsection 2.1. This ansatz leads to the norms

$$(19a) \quad \|(v, \tau)\|_a^2 := \|\tau - \nabla v\|_{L^2(\Omega)}^2 + \|\text{div } \tau\|_{L^2(\Omega)}^2 + \|\text{curl } \tau\|_{L^2(\Omega)}^2,$$

$$(19b) \quad \|(v, \tau)\|_b^2 := \|\nabla v\|_{L^2(\Omega)}^2 + \|\tau\|_{L^2(\Omega)}^2 + \|\text{div } \tau\|_{L^2(\Omega)}^2 + \|\text{curl } \tau\|_{L^2(\Omega)}^2$$

for all $(v, \tau) \in X := H_0^1(\Omega) \times (H(\text{div}, \Omega) \cap H(\text{curl}, \Omega))$ with associated scalar product $a(\bullet, \bullet)$ to $\|\bullet\|_a$ and $b(\bullet, \bullet)$ to $\|\bullet\|_b$.

THEOREM 3.15. (a) *The eigenvalue problem (16) has the eigenpairs $(\mu_j, \phi_j) \in \mathbb{R} \times X$, $j \in \mathbb{N}$, from (15) for the Poisson model problem, and $\mu_0 = 1$ has the eigenspace $\phi_0 \in \{\tau \in H(\text{div}, \Omega) \cap H(\text{curl}, \Omega) : \text{div } \tau = 0\}$.*

(b) *The model problem (19) satisfies (H1)–(H3) and (1).*

Proof. Let $(\lambda_j, \psi_j) \in \mathbb{R} \times H_0^1(\Omega)$, $j \in \mathbb{N}$, denote the eigenpairs of the $-\Delta$ operator. The spectral representation of $H_0^1(\Omega)$ functions and the orthogonal split of Lemma 3.9 lead, for any (u, σ) and (v, τ) in X , to coefficients $u_j, v_j, \sigma_j, \tau_j \in \mathbb{R}$ for $j \in \mathbb{N}$ and zero-divergence functions $\sigma_0, \tau_0 \in H(\text{div}, \Omega) \cap H(\text{curl}, \Omega)$ with

$$u = \sum_{j \in \mathbb{N}} u_j \psi_j, \quad v = \sum_{j \in \mathbb{N}} v_j \psi_j, \quad \sigma = \sigma_0 + \sum_{j \in \mathbb{N}} \sigma_j \nabla \psi_j, \quad \text{and} \quad \tau = \tau_0 + \sum_{j \in \mathbb{N}} \tau_j \nabla \psi_j.$$

As in the proof of Theorem 3.10, this representation results in

$$\begin{aligned} a(u, \sigma; v, \tau) &= \sum_{j \in \mathbb{N}} \begin{pmatrix} u_j \\ \xi_j \end{pmatrix} \cdot \begin{pmatrix} \lambda_j & -\lambda_j \\ -\lambda_j & \lambda_j + \lambda_j^2 \end{pmatrix} \begin{pmatrix} v_j \\ \vartheta_j \end{pmatrix} \\ &\quad + (\sigma_0, \tau_0)_{L^2(\Omega)} + (\text{curl } \sigma_0, \text{curl } \tau_0)_{L^2(\Omega)}, \\ b(u, \sigma; v, \tau) &= \sum_{j \in \mathbb{N}} \begin{pmatrix} u_j \\ \xi_j \end{pmatrix} \cdot \begin{pmatrix} \lambda_j & 0 \\ 0 & \lambda_j + \lambda_j^2 \end{pmatrix} \begin{pmatrix} v_j \\ \vartheta_j \end{pmatrix} \\ &\quad + (\sigma_0, \tau_0)_{L^2(\Omega)} + (\text{curl } \sigma_0, \text{curl } \tau_0)_{L^2(\Omega)}. \end{aligned}$$

The remaining details of the proofs of (a) and (b) follow those in Theorems 3.10 and 3.11 and are omitted for brevity. \square

4. Improved GUB. This section aims at the computation of a guaranteed upper bound (GUB) for the model problems that capture the convergence of $LS(f; U)/\|u - U\|_X^2$ to one.

4.1. A lower bound for the coercivity constant. Estimate (8) indicates that the coercivity constant on the a -orthogonal complement $X(\mathcal{T})^\perp := \{v \in X : \forall W \in X(\mathcal{T}), a(v, W) = 0\}$ of $X(\mathcal{T})$ in X with $\mathcal{T} \in \mathbb{T}$

$$(20) \quad \alpha \leq \alpha(\mathcal{T}) := \inf_{v \in X(\mathcal{T})^\perp \setminus \{0\}} \frac{a(v, v)}{\|v\|_b^2}$$

converges to one as the mesh size tends to zeros. This constant improves the GUB for the exact and discrete LSFEM solution u and U to

$$\|u - U\|_b^2 \leq \alpha(\mathcal{T})^{-1} \|u - U\|_a^2 \leq \alpha^{-1} \|u - U\|_a^2.$$

The aim is the approximation of $\alpha(\mathcal{T})^{-1}$ from above by a constant $C(\mathcal{T})$. The following ansatz requires the smallest discrete eigenvalues $\mu_1(\mathcal{T}) \leq \dots \leq \mu_n(\mathcal{T})$ for a fixed $n \leq \dim X(\mathcal{T})$ with normed eigenfunctions $\Phi_1, \dots, \Phi_n \in X(\mathcal{T})$, that is, $\|\Phi_1\|_b = \dots = \|\Phi_n\|_b = 1$ and

$$(21) \quad \forall j = 1, \dots, n \quad \forall W \in X(\mathcal{T}) \quad a(\Phi_j, W) = \mu_j(\mathcal{T}) b(\Phi_j, W).$$

Furthermore, let $\mu_1 \leq \dots \leq \mu_{n+1}$ be the smallest exact least-squares eigenvalues with eigenfunctions $\phi_1, \dots, \phi_{n+1}$ such that $b(\phi_j, \phi_k) = \delta_{jk}$ for all $j, k = 1, \dots, n+1$, and

$$(22) \quad \forall w \in X \quad a(\phi_j, w) = \mu_j b(\phi_j, w).$$

It follows from **(H2)** that $0 < \mu_1$ and $\{\mu_1, \dots, \mu_{n+1}\} \subset \{\mu(j) : j \in \mathbb{N}\}$. The comparison of exact and discrete eigenvalue clusters in $\{\mu_1, \dots, \mu_n\}$ and $\{\mu_1(\mathcal{T}), \dots, \mu_n(\mathcal{T})\}$ is the basic idea in the computation of $C(\mathcal{T}) \geq \alpha(\mathcal{T})^{-1}$. Therefore, define for any compact interval $[\alpha', \beta'] \subset \mathbb{R}$ the spaces

$$\begin{aligned} E(\alpha', \beta') &:= \overline{\text{span}\{E(\mu(j)) : j \in \mathbb{N}_0, \alpha' \leq \mu(j) \leq \beta'\}} \subset X, \\ E(\alpha', \beta', \mathcal{T}) &:= \text{span}\{\Phi_j : j \in \{1, \dots, n\}, \alpha' \leq \mu_j(\mathcal{T}) \leq \beta'\} \subset X(\mathcal{T}), \end{aligned}$$

and let $[\alpha_1, \beta_1], \dots, [\alpha_m, \beta_m]$ be intervals which satisfy the following hypothesis.

(H4) Let $[\alpha_1, \beta_1], \dots, [\alpha_m, \beta_m]$ be pairwise disjoint compact intervals with $m \leq n$ and $0 < \alpha_1 \leq \alpha \leq \beta_1 < \alpha_2 \leq \beta_2 < \dots \leq \beta_m < \alpha_{m+1}$, which satisfy, for all $\ell = 1, \dots, m$,

$$\dim E(\alpha_\ell, \beta_\ell) = \dim E(\alpha_\ell, \beta_\ell, \mathcal{T}) \quad \text{and} \quad X = E(\alpha_1, \beta_1) \oplus E(\alpha_{\ell+1}, \beta_\ell).$$

The intervals from **(H4)** lead to

$$(23) \quad C(\mathcal{T}) := \alpha_{m+1}^{-1} \left(1 + \sum_{k=1}^m \alpha_{k+1} \frac{\alpha_{m+1} - \alpha_k}{\alpha_k \beta_k} \frac{\beta_k - \alpha_k}{\alpha_{k+1} - \alpha_k} \right).$$

THEOREM 4.1. *Suppose **(H1)**–**(H4)**; then $X(\mathcal{T})^\perp$ from (8) and $C(\mathcal{T})$ satisfy*

$$\forall v \in X(\mathcal{T})^\perp \quad \|v\|_b^2 \leq C(\mathcal{T}) \|v\|_a^2.$$

Remark 4.2. Suppose **(H1)**–**(H4)** and $\alpha_\ell = \mu(\ell)$ for all $\ell = 1, \dots, m+1$ with the smallest pairwise distinct eigenvalues $\mu(1), \mu(2), \dots, \mu(m+1)$ of (3). A small eigenvalue error $\delta := \max_{\ell=1, \dots, m} (\beta_\ell - \mu(\ell))$ of the discrete space guarantees

$$\alpha(\mathcal{T})^{-1} \leq C(\mathcal{T}) = \mu(m+1)^{-1} + O(\delta).$$

Suppose the eigenvalue error is of the form $\delta = O(h_{\max}^s)$ for some rate $s > 0$ and the maximal mesh-size h_{\max} in \mathcal{T} . With a constant $C(m)$, which depends in particular on m , (1) implies

$$(24) \quad \|u - U\|_b^2 / \|u - U\|_a^2 \leq \alpha(\mathcal{T})^{-1} \leq C(\mathcal{T}) \leq \mu(m+1)^{-1} + C(m)h_{\max}^s.$$

Proof of Theorem 4.1. Step 1 (decomposition of $v \in X(\mathcal{T})^\perp$). Given any $v \in X(\mathcal{T})^\perp \setminus \{0\}$, **(H2)** implies $X = E(\alpha_1, \beta_1) \oplus \cdots \oplus E(\alpha_m, \beta_m) \oplus E(\alpha_{m+1}, \beta)$ with $\beta_{m+1} := \beta$ from (2) and so the existence of $v_1, \dots, v_{m+1} \in X$ with $v_j \in E(\alpha_j, \beta_j)$ for all $j = 1, \dots, m+1$ and $v = \sum_{j=1}^{m+1} v_j$. The pairwise orthogonality of the eigenspaces (6) implies that $a(v_j, v_k) = 0 = b(v_j, v_k)$ for all $j, k = 1, \dots, m+1$ with $j \neq k$.

Step 2 (existence of $V_j \in E(\alpha_1, \beta_j, \mathcal{T})$ with $v_j - V_j \in E(\alpha_{j+1}, \beta)$). Let $j \in \{1, \dots, m\}$ and $p = \dim E(\alpha_1, \beta_j)$, so that $\phi_1, \dots, \phi_p \in X$ form a basis of $E(\alpha_1, \beta_j)$. Since $\dim E(\alpha_1, \beta_j) = \dim E(\alpha_1, \beta_j, \mathcal{T})$, there exists a basis $\Phi_1, \dots, \Phi_p \in X(\mathcal{T})$ of $E(\alpha_1, \beta_j, \mathcal{T})$. It holds that $X(\mathcal{T}) \subset X = E(\alpha_1, \beta_j) \oplus E(\alpha_{j+1}, \beta)$. Consequently, there exists a $p \times p$ matrix $B = (B_{k\ell})_{k,\ell=1,\dots,p} \in \mathbb{R}^{p \times p}$ with

$$\forall k = 1, \dots, p \quad \Phi_k - \sum_{\ell=1}^p B_{k\ell} \phi_\ell \in E(\alpha_{j+1}, \beta).$$

To prove that B is invertible, let $\xi = (\xi_1, \dots, \xi_p) \in \mathbb{R}^p$ with $B\xi = 0$. In other words, $\sum_{k=1}^p \xi_k B_{k\ell} = 0$ for all $\ell = 1, \dots, p$. Define

$$W := \xi_1 \Phi_1 + \cdots + \xi_p \Phi_p \in E(\alpha_1, \beta_j, \mathcal{T}).$$

If $\xi \neq 0$, $W \in E(\alpha_1, \beta_j, \mathcal{T}) \setminus \{0\}$ satisfies $a(W, W)/b(W, W) \leq \beta_j$. Furthermore, since

$$\sum_{k=1}^p \xi_k \sum_{\ell=1}^p B_{k\ell} \phi_\ell = \sum_{\ell=1}^p \left(\sum_{k=1}^p \xi_k B_{k\ell} \right) \phi_\ell = 0,$$

it holds that

$$W = W - \sum_{k=1}^p \xi_k \sum_{\ell=1}^p B_{k\ell} \phi_\ell = \sum_{k=1}^p \xi_k \left(\Phi_k - \sum_{\ell=1}^p B_{k\ell} \phi_\ell \right) \in E(\alpha_{j+1}, \beta).$$

This implies $\alpha_{j+1} \leq a(W, W)/b(W, W)$ and contradicts $\beta_j < \alpha_{j+1}$. Therefore, $W = 0$ and $(\xi_1, \dots, \xi_p) = 0$. This proves that B is invertible. Thus, there exist coefficients $b_{\ell 1}, \dots, b_{\ell p} \in \mathbb{R}$ for all $\ell = 1, \dots, p$ with

$$\phi_\ell - \sum_{k=1}^p b_{\ell k} \Phi_k \in E(\alpha_{j+1}, \beta).$$

This implies for $v_j \in \text{span}\{\phi_1, \dots, \phi_p\}$ the existence of $V_j \in \text{span}\{\Phi_1, \dots, \Phi_p\}$ with

$$(25) \quad v_j - V_j \in E(\alpha_{j+1}, \beta) \quad \text{and} \quad V_j \in E(\alpha_1, \beta_j, \mathcal{T}).$$

Step 3 (upper bound for $\|V_j\|_b^2$). It follows from $E(\alpha_1, \beta_j) \perp_a E(\alpha_{j+1}, \beta)$ and $E(\alpha_1, \beta_j) \perp_b E(\alpha_{j+1}, \beta)$ that for V_j from Step 2 the Pythagoras theorem, $\|v_j\|_a^2 = \|V_j\|_a^2 - \|v_j - V_j\|_a^2$ and $\|v_j - V_j\|_b^2 = \|V_j\|_b^2 - \|v_j\|_b^2$, holds. Since $V_j \in E(\alpha_1, \beta_j, \mathcal{T})$, it holds that $\|V_j\|_a^2 \leq \beta_j \|V_j\|_b^2$. Moreover, $v_j - V_j \in E(\alpha_{j+1}, \beta)$ implies $\alpha_{j+1} \|v_j - V_j\|_b^2 \leq \|v_j - V_j\|_a^2$, $v_j \in E(\alpha_j, \beta_j)$ induces $\alpha_j \|v_j\|_b^2 \leq \|v_j\|_a^2$. This leads to

$$\alpha_j \|v_j\|_b^2 \leq \|v_j\|_a^2 = \|V_j\|_a^2 - \|v_j - V_j\|_a^2 \leq \beta_j \|V_j\|_b^2 - \alpha_{j+1} (\|V_j\|_b^2 - \|v_j\|_b^2).$$

Consequently,

$$(26) \quad \|V_j\|_b^2 \leq \frac{\alpha_{j+1} - \alpha_j}{\alpha_{j+1} - \beta_j} \|v_j\|_b^2.$$

Step 4 (upper bound for $\|v_j\|_a^2$). Case 1. Let $v_j \neq 0$. This step utilizes $a(v_j, v_j - V_j) = 0 = a(v, V_j)$ and a Cauchy-Schwarz inequality to deduce

$$\|v_j\|_a^2 = a(v, v_j) = a(v, v_j - V_j) = a(v - v_j, v_j - V_j) \leq \|v - v_j\|_a \|v_j - V_j\|_a.$$

The combination with the Pythagoras theorem, $\|v - v_j\|_a^2 = \|v\|_a^2 - \|v_j\|_a^2$ and $\|v_j - V_j\|_a^2 = \|V_j\|_a^2 - \|v_j\|_a^2$, leads to $\|v\|_a^2 \|v_j\|_a^2 + \|v_j\|_a^2 \|V_j\|_a^2 \leq \|v\|_a^2 \|V_j\|_a^2$. Given $v_j \neq 0$, it follows from $v_j - V_j \in E(\alpha_{j+1}, \beta)$ and $E(\alpha_j, \beta_j) \cap E(\alpha_{j+1}, \beta) = \{0\}$ from (25) that $V_j \neq 0$. Consequently, the division of the previous estimate by $\|v\|_a^2 \|v_j\|_a^2 \|V_j\|_a^2 \neq 0$ results in

$$(27) \quad \|v\|_a^{-2} + \|V_j\|_a^{-2} \leq \|v_j\|_a^{-2}.$$

Since $V_j \in E(\alpha_j, \beta_j, \mathcal{T})$ and $v_j \in E(\alpha_j, \beta_j)$ fulfill $\beta_j^{-1} \|V_j\|_b^{-2} \leq \|V_j\|_a^{-2}$ and $\|v_j\|_a^{-2} \leq \alpha_j^{-1} \|v_j\|_b^{-2}$, (26) leads in (27) to

$$(28) \quad \|v_j\|_b^2 \leq \left(\frac{1}{\alpha_j} - \frac{\alpha_{j+1} - \beta_j}{\beta_j(\alpha_{j+1} - \alpha_j)} \right) \|v\|_a^2.$$

Case 2. The estimate (28) is trivial for $v_j = 0$.

Step 5 (lower bound for $\|v\|_a^2$). The estimate $\alpha_j \|v_j\|_b^2 \leq \|v_j\|_a^2$ for all $j = 1, \dots, m+1$ and the pairwise a - and b -orthogonality of v_1, \dots, v_{m+1} prove

$$(29) \quad \sum_{j=1}^m \alpha_j \|v_j\|_b^2 + \alpha_{m+1} \left(\|v\|_b^2 - \sum_{j=1}^m \|v_j\|_b^2 \right) \leq \sum_{j=1}^{m+1} \|v_j\|_a^2 = \|v\|_a^2.$$

Since $\alpha_j - \alpha_{m+1} < 0$, the lower bound decreases monotonically in $\|v_j\|_b^2$ for each $j = 1, \dots, m$ and fixed $\|v\|_b^2$. Hence, the substitution of (28) into (29) leads to

$$\begin{aligned} \alpha_{m+1} \|v\|_b^2 &\leq \|v\|_a^2 + \sum_{j=1}^m (\alpha_{m+1} - \alpha_j) \left(\frac{1}{\alpha_j} - \frac{\alpha_{j+1} - \beta_j}{\beta_j(\alpha_{j+1} - \alpha_j)} \right) \|v\|_a^2 \\ &= \left(1 + \sum_{j=1}^m \alpha_{j+1} \frac{\alpha_{m+1} - \alpha_j}{\alpha_j \beta_j} \frac{\beta_j - \alpha_j}{\alpha_{j+1} - \alpha_j} \right) \|v\|_a^2. \quad \square \end{aligned}$$

4.2. Numerical realization. The application of Theorem 4.1 for the model problems runs a three-stage algorithm.

Stage 1. Compute $N + 1$ lower bounds $0 < \mu_1^{\text{low}} \leq \dots \leq \mu_{N+1}^{\text{low}}$ for the smallest continuous eigenvalues in (16) (resp., (18)), i.e. $\mu_j^{\text{low}} \leq \mu_j$ for $j = 1, \dots, N + 1$. This computation is independent of the current triangulation and done offline. The numerical experiments in this paper adopt [1, 12] as detailed in section 5.

Stage 2. Given a triangulation $\mathcal{T} \in \mathbb{T}$, compute upper bounds for the smallest discrete least-squares eigenvalues $0 < \mu_1(\mathcal{T}) \leq \dots \leq \mu_N(\mathcal{T})$ with linear independent eigenfunctions $\Phi_1, \dots, \Phi_N \in X(\mathcal{T}) \setminus \{0\}$ such that

$$(30) \quad \forall \ell = 1, \dots, N \quad \forall W \in X(\mathcal{T}) \quad a(\Phi_\ell, W) = \mu_\ell(\mathcal{T}) b(\Phi_\ell, W).$$

This leads to $\mu_1^{\text{up}}(\mathcal{T}) \leq \dots \leq \mu_N^{\text{up}}(\mathcal{T})$ with $\mu_\ell(\mathcal{T}) \leq \mu_\ell^{\text{up}}(\mathcal{T})$ for all $\ell = 1, \dots, N$. The MATLAB function `eigs` (with standard parameters) solves (30) in section 5 and achieves $\mu_\ell^{\text{up}}(\mathcal{T}) = \mu_\ell(\mathcal{T})$ for all $\ell = 1, \dots, N$.

Stage 3. Given the lower and upper eigenvalue bounds from Stages 1 and 2, compute $C(\mathcal{T})$ for all $n = 0, \dots, N$ via the subsequent routine

- (i) set $\alpha_1 := \mu_1^{\text{low}}$ and $m := 0$;
- (ii) **for** $k = 1, \dots, n$,
 if $\mu_k^{\text{up}}(\mathcal{T}) < \mu_{k+1}^{\text{low}}$ **then** set $m := m + 1$, $\beta_m := \mu_k^{\text{up}}(\mathcal{T})$, $\alpha_{m+1} := \mu_{k+1}^{\text{low}}$;
- (iii) apply the formula (23);

Output: The minimum $C(\mathcal{T})$ of the values from (iii) for $n = 0, \dots, N$

PROPOSITION 4.3. *The three-stage algorithm leads to $C(\mathcal{T})$ in Theorem 4.1.*

Proof. It suffices to show that the values $\alpha_1, \dots, \alpha_{m+1}$ and β_1, \dots, β_m from (i) and (ii) in Stage 3 with $n = 0, \dots, N$ satisfy **(H4)** for all $\ell = 1, \dots, m$. Then Theorem 4.1 applies to all $n = 0, \dots, N$ and results in the GUB.

Step 1 (proof of $0 < \alpha_1 \leq \alpha \leq \beta_1 < \alpha_2 \leq \beta_2 < \dots \leq \beta_m < \alpha_{m+1}$). For all $j = 1, \dots, n$, the Rayleigh–Ritz principle leads to

$$\mu_j^{\text{low}} \leq \mu_j = \min_{\substack{X_j \subset X \\ \dim X_j = j}} \max_{\substack{v \in X_j \\ \|v\|_b = 1}} a(v, v) \leq \mu_j(\mathcal{T}) = \min_{\substack{X_j(\mathcal{T}) \subset X(\mathcal{T}) \\ \dim X_j(\mathcal{T}) = j}} \max_{\substack{V \in X_j(\mathcal{T}) \\ \|V\|_b = 1}} a(V, V) \leq \mu_j^{\text{up}}(\mathcal{T}).$$

This proves $0 < \alpha_1 = \mu_1^{\text{low}} \leq \mu_1 = \alpha \leq \mu_1^{\text{up}}(\mathcal{T}) = \beta_1$. Moreover, for all $\ell = 1, \dots, m$ there exists a $k \in \{1, \dots, n\}$ such that $\beta_\ell = \mu_k^{\text{up}}(\mathcal{T}) < \mu_{k+1}^{\text{low}} = \alpha_{\ell+1}$. If $\ell < m$, it also holds that $\alpha_{\ell+1} = \mu_{k+1}^{\text{low}} \leq \mu_{k+1}^{\text{up}}(\mathcal{T}) \leq \beta_{\ell+1}$.

Step 2 (proof of $\dim E(\alpha_\ell, \beta_\ell) = \dim E(\alpha_\ell, \beta_\ell, \mathcal{T})$). Given an interval $[\alpha_\ell, \beta_\ell]$ with $\ell = 1, \dots, m$, let $\ell_1 \in \{1, \dots, n\}$ be the smallest index with $\alpha_\ell = \mu_{\ell_1}^{\text{low}}$ and $\ell_2 \in \{\ell_1, \dots, n\}$ the biggest index with $\beta_\ell = \mu_{\ell_2}^{\text{up}}(\mathcal{T})$. Then

$$\alpha_\ell = \mu_{\ell_1}^{\text{low}} \leq \mu_{\ell_1} \leq \mu_{\ell_1+1} \leq \dots \leq \mu_{\ell_2} \leq \mu_{\ell_2}^{\text{up}}(\mathcal{T}) = \beta_\ell$$

implies $\ell_2 - \ell_1 + 1 \leq \dim E(\alpha_\ell, \beta_\ell)$. If $\ell_2 - \ell_1 + 1 < \dim E(\alpha_\ell, \beta_\ell)$, there exists an eigenpair $(\mu, \phi) \in [\alpha_\ell, \beta_\ell] \times X \setminus \{0\}$ with $a(\phi, w) = \mu b(\phi, w)$ for all $w \in X$ and $b(\phi, \phi_k) = 0$ for all $k = 1, \dots, n + 1$. The eigenvalue μ is strictly smaller than μ_{ℓ_2+1} . This contradicts the assumption that μ_1, \dots, μ_{n+1} are the smallest eigenvalues. Therefore, $\dim E(\alpha_\ell, \beta_\ell) = \ell_2 - \ell_1 + 1$. Similar arguments lead to $\dim E(\alpha_\ell, \beta_\ell, \mathcal{T}) = \ell_2 - \ell_1 + 1$.

Step 3 (proof of $X = E(\alpha_1, \beta_\ell) \oplus E(\alpha_{\ell+1}, \beta)$). For all $\ell = 1, \dots, m$ there exists $k \in \{1, \dots, n\}$ with $\mu_k \leq \mu_k^{\text{up}}(\mathcal{T}) = \beta_\ell < \alpha_{\ell+1} = \mu_{k+1}^{\text{low}} \leq \mu_{k+1}$. Let $\phi_j \in E(\mu(j))$ with $j \in \mathbb{N}$. Since μ_1, \dots, μ_n are the smallest eigenvalues with (22), it holds that either $\mu(j) \leq \mu_k$ or $\mu_{k+1} \leq \mu(j)$. This reveals $\phi_j \in E(\alpha_1, \beta_\ell)$ or $\phi_j \in E(\alpha_{\ell+1}, \beta)$. Therefore, any eigenfunction belongs to $E(\alpha_1, \beta_\ell) \oplus E(\alpha_{\ell+1}, \beta)$. The density of the linear hull of eigenfunctions in X from **(H2)** implies $X = E(\alpha_1, \beta_\ell) \oplus E(\alpha_{\ell+1}, \beta)$. \square

Remark 4.4. It follows from the Rayleigh–Ritz principle that $\mu_1^{\text{up}}(\mathcal{T}), \dots, \mu_N^{\text{up}}(\mathcal{T})$ are upper bounds for the smallest discrete eigenvalues in (30) for any discrete space $\hat{X}(\mathcal{T})$ with $X(\mathcal{T}) \subset \hat{X}(\mathcal{T})$. Thus, the GUB $C(\mathcal{T})LS(f; \hat{U})$ holds for the solution \hat{U} to the LSFEM with any discrete space $\hat{X}(\mathcal{T})$ with $X(\mathcal{T}) \subset \hat{X}(\mathcal{T})$. This enables the possibility of applying (adaptive) *hp*-refinements.

5. Numerical experiments. This section underlines the theoretical results of this paper with numerical experiments for the Poisson model problem, the Helmholtz equation, and the Maxwell equations and exploits its efficiency.

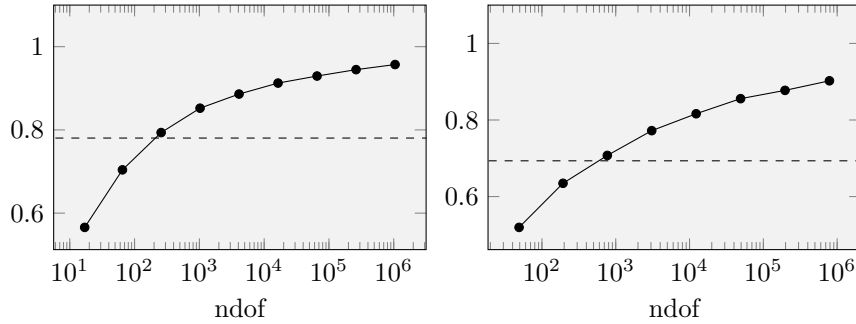


FIG. 2. Coercivity constant α (dashed line) and $C(\mathcal{T})^{-1}$ on the unit square (left) and the L-shaped domain (right) in the Poisson model problem.

5.1. Asymptotic exactness in the Poisson model problem. The first experiment is displayed in Table 1 and investigates the asymptotic exactness of the residual $LS(f; u_C, p_{RT})$ with the discrete solution $(u_C, p_{RT}) \in X(\mathcal{T}) := S_0^1(\mathcal{T}) \times RT_0(\mathcal{T})$ to the Poisson model problem on the L-shaped domain with constant right-hand side $f \equiv 1$ on uniformly refined meshes. The exact solution $(u, p) \in X$ to the problem is unknown, but the computation of reference solutions on finer grids results in guaranteed upper and lower bounds for the error $\|(u, p) - (u_C, p_{RT})\|_X$; details can be found in section SM2 of the supplementary material. The outcome verifies the convergence of the ratio $LS(f; u_C, p_{RT}) / \|(u, p) - (u_C, p_{RT})\|_X^2$ to one and confirms (1). This is also observed in other numerical examples outlined in section SM3.

5.2. Improved GUB for the Poisson model problem. This experiment exploits the improvement of the error estimation with the three-stage algorithm from subsection 4.2 with $N = 60$. It solves the Poisson model problem with $X(\mathcal{T}) := S_0^1(\mathcal{T}) \times RT_0(\mathcal{T})$ on uniformly refined grids. The lower least-squares eigenvalue bounds from Stage 1 utilize the Crouzeix–Raviart–FEM (see section SM4 of the supplementary material for details), which applies on the fly on each triangulation \mathcal{T} . The upper bounds for the discrete eigenvalues in Stage 2 are computed with the MATLAB function `eigs`. The required CPU time for the first 60 eigenvalues in the algebraic eigenvalue problem is approximately 15 times larger than the CPU time for one solve of the LS-FEM with the MATLAB function `mldivide`. Figure 2 displays the result for the square and the L-shaped domain and visualizes the convergence of $C(\mathcal{T})$ (and so of $\alpha(\mathcal{T})$) to one as well as the improvement of the GUB $\|u - U\|_X^2 \leq C(\mathcal{T}) LS(f; U)$ compared with the classical GUB $\|u - U\|_X^2 \leq \alpha^{-1} LS(f; U)$ with coercivity constant α from (2). On the finest mesh the improvements read $C(\mathcal{T}) = 1.044854 \leq \alpha^{-1} = 1.281371$ on the square domain and $C(\mathcal{T}) = 1.108241 \leq \alpha^{-1} = 1.442114$ on the L-shaped domain.

5.3. Improved GUB for the Helmholtz equation. This subsection investigates the three-stage algorithm from subsection 4.2 with $N = 60$ for the Helmholtz equation with $X(\mathcal{T}) := S_0^1(\mathcal{T}) \times RT_0(\mathcal{T})$ on the square domain $\Omega = (0, 1)^2$ and on the L-shaped domain $\Omega = (-1, 1)^2 \setminus [0, 1]^2$ with uniformly refined meshes. The lowest-order Courant-FEM computes upper eigenvalue bounds for λ_k and the Crouzeix–Raviart-FEM computes lower eigenvalue bounds for λ_k . If the lower eigenvalue bound for λ_k is bigger than ω^2 or the upper eigenvalue bound for λ_k is smaller than ω^2 , it leads to a lower bound for the least-squares eigenvalue in Table 3. Otherwise, the approach fails (this leads to the missing data in Figure 4). Figure 3 plots $C(\mathcal{T})^{-1}$

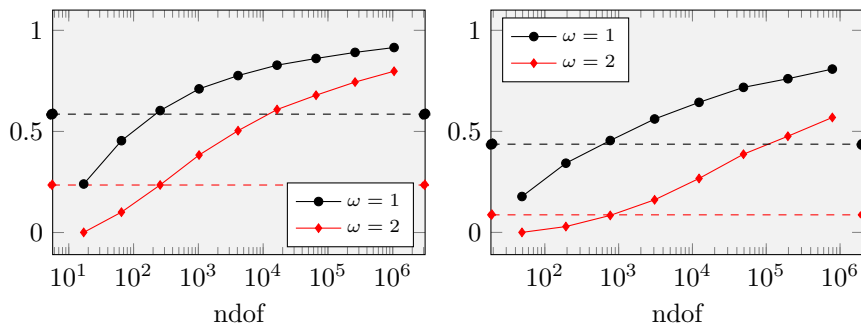


FIG. 3. Coercivity constant α (dashed line) and $C(\mathcal{T})^{-1}$ on the unit square (left) and the L-shaped domain (right) in the Helmholtz equation.

for $\omega = 1$ and $\omega = 2$. It indicates the convergence of $C(\mathcal{T})^{-1}$ (and so of $\alpha(\mathcal{T})$) to one. The reliability constant $C(\mathcal{T})$ improves the classical reliability constant α^{-1} on the finest grid as follows: $C(\mathcal{T}) = 1.093083 \leq \alpha^{-1} = 1.708149$ on the square domain with $\omega = 1$, $C(\mathcal{T}) = 1.253660 \leq \alpha^{-1} = 4.256367$ on the square domain with $\omega = 2$, $C(\mathcal{T}) = 1.237410 \leq \alpha^{-1} = 2.290786$ on the L-shaped domain with $\omega = 1$, $C(\mathcal{T}) = 1.758341 \leq \alpha^{-1} = 11.521603$ on the L-shaped domain with $\omega = 2$.

5.4. Improved GUB for the Helmholtz equation with large frequencies. Table 4 compares the reliability constant α^{-1} (computed with the Dirichlet eigenvalues of $-\Delta$ from [21] and [17]) with the reliability constant $C(\mathcal{T})$ (computed with the three-stage algorithm from subsection 4.2) for the Helmholtz equation of subsection 5.3 with frequencies $\omega = 0, \dots, 10$. For frequencies $\omega \geq 7$ the computation leads to $C(\mathcal{T})$ close to α^{-1} . In other words, the improvement of the GUB with the three-stage algorithm was negligible. To study the efficiency of the GUB $C(\mathcal{T})LS(f;U)$, Figure 4 and Table 5 compare the residual and the exact error of the LSFEM for the Helmholtz equation on the unit square with $\omega = 4$ and known solution $(\sin(\pi x) \sin(\pi y), \nabla \sin(\pi x) \sin(\pi y))$ as well as with $\omega = 7$ and known solution $(\sin(2\pi x) \sin(\pi y), \nabla \sin(2\pi x) \sin(\pi y))$. The experiment indicates that the GUB $\alpha^{-1}LS(f;U)$ is indeed an accurate upper bound in the preasymptotic regime and cannot be improved by $C(\mathcal{T})$. However, for finer triangulations and small frequencies such as $\omega = 4$, the GUB $C(\mathcal{T})LS(f;U)$ captures the fast decay of the error and results in an improvement by several orders of magnitude and so justifies the higher CPU time as discussed in subsection 5.7. For large frequencies $\omega \geq 7$, the FEM does not resolve the highly oscillating eigenfunctions in the computational domain of this experiment. This provides numerical evidence for an efficient error control despite the fact that the constant is far away from one in the preasymptotic regime. The limited memory of the computer does not allow us to determine the constant $C(\mathcal{T})$ on finer grids than the nine times uniformly refined mesh \mathcal{T}_9 , and so $C(\mathcal{T}_9)$ is applied to finer meshes as well with reduced efficiency.

5.5. Improved GUB for the Maxwell equations. The three-stage algorithm from subsection 4.2 is run with $N = 20$ to the Maxwell LSFEM with $X(\mathcal{T}) = \mathcal{N}_0^0(\mathcal{T}) \times \mathcal{N}^0(\mathcal{T})$ on the cube domain $\Omega = (0, 1)^3$ and the Fichera corner domain $\Omega = (-1, 1)^3 \setminus [0, 1]^3$. The lower eigenvalue bounds in Stage 1 are taken from the exact Maxwell eigenvalues λ_j on the cube domain from [16]. The upper and lower eigenvalue bounds for λ_j on the Fichera corner domain from [1] lead with the identities in Table 3 to

TABLE 4

Reliability constants $C(\mathcal{T})$ and α^{-1} in the Helmholtz equation on the uniformly refined unit square with $\text{ndof} = 1048577$, $h_{\max} = 2^{-15/2}$ (left) and the L-shaped domain with $\text{ndof} = 786433$, $h_{\max} = 2^{-13/2}$ (right).

ω	$C(\mathcal{T})$	α^{-1}	ω	$C(\mathcal{T})$	α^{-1}
0	1.04485379	1.28137056	0	1.10824134	1.44211422
1	1.09308333	1.70814860	1	1.23740999	2.29078585
2	1.25365982	4.25636803	2	1.75834047	11.5216028
3	1.58732441	21.4998095	3	2.34866936	2607.01809
4	3.32921432	438.219776	4	7.40823054	7198.38756
5	4.73101753	497.903825	5	193.267713	1021.20011
6	8.98796502	394.084011	6	1319.38306	2678.88237
7	1010101.01	1041666.66	7	1204819.28	1041666.67
8	160.287234	1520.40382	8	151285.930	-
9	90171.3255	128700.129	9	125786.164	-
10	558659.22	598802.395	10	609756.098	-

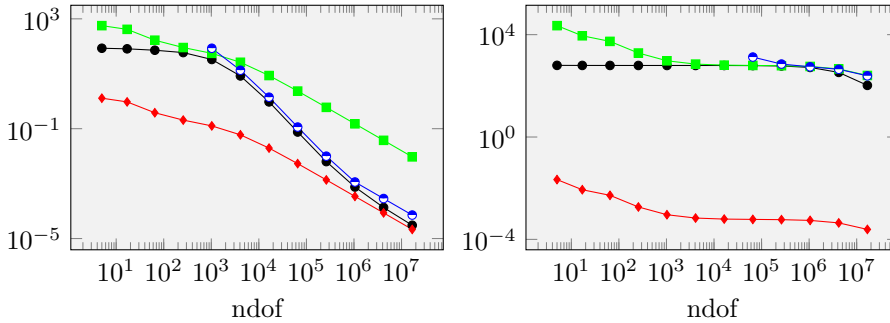


FIG. 4. Error $\|u - U\|_X^2$ (\bullet), residual $LS(f; U)$ (\blacklozenge), GUB $LS(f; U)/\alpha$ (\blacksquare), and GUB $C(\mathcal{T})LS(f; U)$ (\bullet) in the Helmholtz equation with $\omega = 4$ (left) and $\omega = 7$ (right).

TABLE 5

$I_{\text{eff}}(C(\mathcal{T})) := C(\mathcal{T})^{1/2}LS(f; U)^{1/2}/\|u - U\|_X$ and $I_{\text{eff}}(\alpha) := \alpha^{-1/2}LS(f; U)^{1/2}/\|u - U\|_X$.

ndof	$\omega = 4$		$\omega = 7$	
	$I_{\text{eff}}(C(\mathcal{T}))$	$I_{\text{eff}}(\alpha)$	$I_{\text{eff}}(C(\mathcal{T}))$	$I_{\text{eff}}(\alpha)$
257	33.44	1.23	-	1.75
1025	1.60	1.29	-	1.24
4097	1.27	1.77	-	1.06
16385	1.22	3.02	-	1.02
65537	1.23	5.56	1.47	1.01
262145	1.25	9.72	1.09	1.01
1048577	1.23	14.15	1.03	1.05
4194305	1.46	16.70	1.15	1.17
16777217	1.53	17.60	1.54	1.56

lower eigenvalue bounds for the Fichera corner domain. Table 6 shows a preasymptotic regime with $C(\mathcal{T})$ and α^{-1} close ($C(\mathcal{T}) = \alpha^{-1}$ on the coarsest mesh) together without significant improvement of $C(\mathcal{T})$. As $h_{\max} \ll 1$ decreases, the values $C(\mathcal{T})$ decrease and lead to a smaller reliability constant.

5.6. Convergence speed. Remark 4.2 states that with a fixed number N of approximated eigenvalues the constant $C(\mathcal{T})^{-1}$ converges toward the inverse μ_{N+1}^{-1} of the $N+1$ smallest least-squares eigenvalue μ_{N+1} in (16) (resp., (18)). The convergence speed depends on the convergence speed of the eigenvalue bounds toward the exact

TABLE 6
 $C(\mathcal{T})$ for $\omega = 1$ and $\omega = 2$ on the unit cube (left) and Fichera corner domain (right).

ndof	$\omega = 1$	$\omega = 2$	ndof	$\omega = 1$	$\omega = 2$
106	1.749637	5.433454	96	7.005450	282.3264
772	1.673570	5.328303	682	6.519202	282.3264
6024	1.494625	4.071214	5284	4.981221	279.1736
47888	1.372395	2.962454	41928	3.746034	261.4379
382496	1.297562	2.269467	334736	3.066027	232.3960

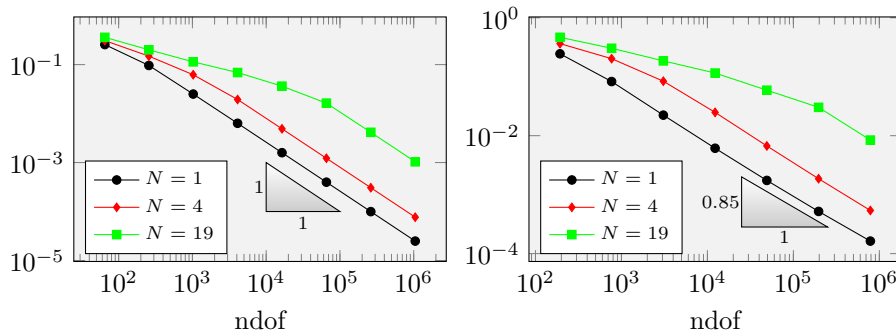


FIG. 5. Distance $\mu_{N+1}^{-1} - C(\mathcal{T})$ in the Poisson model problem on the unit square (left) and the L-shaped domain (right).

eigenvalues. This leads to $C(\mathcal{T}) - \mu_{N+1}^{-1} = \mathcal{O}(h_{\max}^2)$ for the Poisson model problem on the unit square. The reduced elliptic regularity on the L-shaped domain results for the Poisson model problem in the reduced convergence speed $C(\mathcal{T}) - \mu_{N+1}^{-1} = \mathcal{O}(h_{\max}^{2-\epsilon})$ with $\epsilon > 0$ and an educated guess $\epsilon = 2/3$. Figure 5 displays the distance $C(\mathcal{T}) - \mu_{N+1}^{-1}$ from a computation as in subsection 5.2 with fixed $N = 1, 4, 19$ and uniformly refined meshes. It confirms the expected convergence rate on the unit square. On the L-shaped domain, the displayed convergence speed equals $\mathcal{O}(h_{\max}^{1.7})$ for $N = 1, 4$ and differs from the expected rate $\mathcal{O}(h_{\max}^{4/3})$. This might indicate that the computation with up to $\text{ndof} = 1048577$ degrees of freedom does not overcome the preasymptotic regime. For the same reason, no convergence rate can be observed for $N = 19$ on the L-shaped domain.

5.7. Discussion. The overall conclusions from all the numerical benchmarks reported in this section are in agreement with the theoretical predictions of this work. The improvement of the reliability constant $\alpha C(\mathcal{T})$ is visible in all experiments and moderate for the Poisson model problem without degenerated geometry but can exceed several orders of magnitude for certain parameters of ω in the Helmholtz and Maxwell equations. A possible explanation starts with the overall observation that $\|u - U\|_X^2 \leq LS(f; U)$ in (1) so that $1 \leq C(\mathcal{T}) \leq \alpha^{-1}$ and α^{-1} moderate merely implies a moderate improvement of $\alpha C(\mathcal{T}) \leq 1$. For critical parameter $2 \leq \omega \leq 6$ in subsection 5.4, Table 4 displays $4 \leq \alpha^{-1} \leq 500$ and allows for a dramatic improvement of $\alpha C(\mathcal{T}) \ll 1$. In those examples, a few eigenfunctions need to be resolved (with h_{\max} sufficiently small) so that (24) leads to $C(\mathcal{T})$ close to $\mu(m+1)^{-1} \ll \mu(1)^{-1} = \alpha^{-1}$ with a moderate $m \in \mathbb{N}$. This reduction factor of nearly $\alpha \mu(m+1)^{-1}$ for fine meshes has to be evaluated in relation to the additional costs for several eigenvalue calculations.

The remaining parts of this subsection focus on the guaranteed error control as a stopping criterion of an adaptive mesh-refinement with guaranteed control of $\|u -$

$U\|_X$ smaller than a given tolerance tol . Suppose that a fine triangulation \mathcal{T} satisfies $C(\mathcal{T})LS(f;U) \leq \text{tol}^2$ with ndof degrees of freedom in the discrete system. For a simplified comparison, suppose that the computational costs CPU are proportional to ndof (for an optimal iterative solver despite the fact that our numerical examples run with the direct MATLAB solver `mldivide`). Subsection 5.2 suggests that the adaptive algorithm may stop with the triangulation \mathcal{T} , but requires extra costs of 15 CPU for the more expansive improved GUB; the final result is obtained with the costs 16 CPU (online) with the application of the three-stage algorithm of subsection 4.2. In the present model situation, the usage of $\alpha^{-1}LS(f;U)$ implies further mesh-refinements until the bound $\alpha^{-1}LS(f;U') \leq \text{tol}^2$ holds for a discrete solution U' with respect to a much finer mesh \mathcal{T}' with ndof' degrees of freedom. In the case of low-order discretizations at hand and an optimal convergence rate 0.5 of the adaptive algorithm in 2D, one may expect $\alpha \text{ndof}' = \text{ndof}/C(\mathcal{T})$. The computational costs of the discrete solutions with respect to \mathcal{T}' are larger than $\alpha^{-1}C(\mathcal{T})^{-1}$. Hence, if $\alpha C(\mathcal{T}) \leq 1/16$, the three-stage algorithm of subsection 4.2 appears less expensive in the computational online costs. This calculation leaves out the additional mesh-refinements required in the adaptive algorithm to compute \mathcal{T}' and therefore is very conservative. This discussion also ignores the fact that $C(\tilde{\mathcal{T}})$ may be computed on a moderate mesh $\tilde{\mathcal{T}}$ and may utilize $C(\mathcal{T}) \leq C(\tilde{\mathcal{T}})$ for all refinements \mathcal{T} .

The offline costs concern the eigenvalues of the domain, which are known in subsection 5.5 and are less laborious in subsections 5.2–5.4: the convergence rate $O(h_{\max}^{2s})$ of the eigenvalue error is of higher order compared to $O(h_{\max}^s)$ in the source problem for $s \leq 1$ depending on the reduced elliptic regularity.

Based on this discussion, the three-stage algorithm of subsection 4.2 is advantageous in subsection 5.4 for $3 \leq \omega \leq 6$ (and for higher ω with much finer meshes). As a rule of thumb, the proposed algorithm appears advantageous if $16\alpha \leq \mu(m+1)$ for moderate m and sufficiently small tolerances in guaranteed error control.

Acknowledgments. The work was written while the authors enjoyed the hospitality of the Hausdorff Research Institute of Mathematics in Bonn, Germany, during the Hausdorff Trimester Program “Multiscale Problems: Algorithms, Numerical Analysis and Computation”. The constructive suggestions of the anonymous referees led to an improved revision and in particular to the addition of subsections 3.3 and 5.7.

REFERENCES

- [1] G. R. BARRENECHEA, L. BOULTON, AND N. BOUSSAÏD, *Local two-sided bounds for eigenvalues of self-adjoint operators*, Numer. Math., 135 (2017), pp. 953–986, <https://doi.org/10.1007/s00211-016-0822-1>.
- [2] P. BOCHEV AND M. GUNZBURGER, *On least-squares finite element methods for the Poisson equation and their connection to the Dirichlet and Kelvin principles*, SIAM J. Numer. Anal., 43 (2005), pp. 340–362, <https://doi.org/10.1137/S003614290443353X>.
- [3] P. B. BOCHEV AND M. D. GUNZBURGER, *Least-Squares Finite Element Methods*, Appl. Math. Sci. 166, Springer, New York, 2009, <https://doi.org/10.1007/b13382>.
- [4] D. BOFFI, F. BREZZI, AND M. FORTIN, *Mixed Finite Element Methods and Applications*, Springer Ser. Comput. Math. 44, Springer, Heidelberg, 2013, <https://doi.org/10.1007/978-3-642-36519-5>.
- [5] D. BRAESS, *Finite Elements. Theory, Fast Solvers, and Applications in Elasticity Theory*, 3rd ed., Cambridge University Press, Cambridge, UK, 2007.
- [6] J. H. BRAMBLE, T. V. KOLEV, AND J. E. PASCIAK, *A least-squares approximation method for the time-harmonic Maxwell equations*, J. Numer. Math., 13 (2005), pp. 237–263, <https://doi.org/10.1163/156939505775248347>.

- [7] S. C. BRENNER AND L. R. SCOTT, *The Mathematical Theory of Finite Element Methods*, Texts Appl. Math. 15, 3rd ed., Springer, New York, 2008, <https://doi.org/10.1007/978-0-387-75934-0>.
- [8] Z. CAI, V. CAREY, J. KU, AND E.-J. PARK, *Asymptotically exact a posteriori error estimators for first-order div least-squares methods in local and global L_2 norm*, *Comput. Math. Appl.*, 70 (2015), pp. 648–659, <https://doi.org/10.1016/j.camwa.2015.05.010>.
- [9] Z. CAI, J. KORSawe, AND G. STARKE, *An adaptive least squares mixed finite element method for the stress-displacement formulation of linear elasticity*, *Numer. Methods Partial Differential Equations*, 21 (2005), pp. 132–148, <https://doi.org/10.1002/num.20029>.
- [10] Z. CAI, R. LAZAROV, T. A. MANTEUFFEL, AND S. F. MCCORMICK, *First-order system least squares for second-order partial differential equations: Part I*, *SIAM J. Numer. Anal.*, 31 (1994), pp. 1785–1799, <https://doi.org/10.1137/0731091>.
- [11] Z. CAI, T. A. MANTEUFFEL, AND S. F. MCCORMICK, *First-order system least squares for second-order partial differential equations: Part II*, *SIAM J. Numer. Anal.*, 34 (1997), pp. 425–454, <https://doi.org/10.1137/S0036142994266066>.
- [12] C. CARSTENSEN AND J. GEDICKE, *Guaranteed lower bounds for eigenvalues*, *Math. Comp.*, 83 (2014), pp. 2605–2629, <https://doi.org/10.1090/S0025-5718-2014-02833-0>.
- [13] C. L. CHANG, *Finite element approximation for grad-div type systems in the plane*, *SIAM J. Numer. Anal.*, 29 (1992), pp. 452–461, <https://doi.org/10.1137/0729027>.
- [14] P. G. CIARLET, *Mathematical Elasticity. Vol. I. Three-Dimensional Elasticity*, *Stud. Math. Appl.* 20, North-Holland, Amsterdam, 1988.
- [15] P. G. CIARLET AND J.-L. LIONS, EDs., *Handbook of Numerical Analysis. Vol. II. Finite Element Methods. Part 1*, North-Holland, Amsterdam, 1991.
- [16] M. COSTABEL AND M. DAUGE, *Maxwell Eigenmodes in Tensor Product Domains*, <https://perso.univ-rennes1.fr/monique.dauge/publis/CoDa06MaxTens2.pdf>, 2006.
- [17] D. GALLISTL, *Adaptive Finite Element Computation of Eigenvalues*, doctoral dissertation, Humboldt-Universität zu Berlin, Mathematisch-Naturwissenschaftliche Fakultät II, 2014, <http://edoc.hu-berlin.de/docviews/abstract.php?id=40852>.
- [18] B.-N. JIANG AND L. A. POVINELLI, *Optimal least-squares finite element method for elliptic problems*, *Comput. Methods Appl. Mech. Engrg.*, 102 (1993), pp. 199–212, [https://doi.org/10.1016/0045-7825\(93\)90108-A](https://doi.org/10.1016/0045-7825(93)90108-A).
- [19] P. MONK, *Finite Element Methods for Maxwell's Equations*, *Numer. Math. Sci. Comput.*, Oxford University Press, New York, 2003, <https://doi.org/10.1093/acprof:oso/9780198508885.001.0001>.
- [20] A. I. PEHLIVANOV, G. F. CAREY, AND R. D. LAZAROV, *Least-squares mixed finite elements for second-order elliptic problems*, *SIAM J. Numer. Anal.*, 31 (1994), pp. 1368–1377, <https://doi.org/10.1137/0731071>.
- [21] L. N. TREFETHEN AND T. BETCKE, *Computed eigenmodes of planar regions*, in *Recent Advances in Differential Equations and Mathematical Physics*, *Contemp. Math.* 412, AMS, Providence, RI, 2006, pp. 297–314, <https://doi.org/10.1090/conm/412/07783>.